DEPARTMENT OF COMMERCE
LEWIS L. STRAUSS, Secretary

WEATHER BUREAU
F. W. REICHELDERFER, Chief

MONTHLY WEATHER REVIEW

JAMES E. CASKEY, JR., Editor

Volume 87
Number 1

JANUARY 1959

Closed March 15, 1959
Issued April 15, 1959

THE MAUNA LOA HIGH-ALTITUDE OBSERVATORY

SAUL PRICE

U.S. Weather Bureau, Honolulu, Hawaii

and

JACK C. PALES

U.S. Weather Bureau, Mauna Loa Observatory, Hawaii

[Manuscript received October 6, 1958; revised March 12, 1959]

ABSTRACT

A description is given of the physical setting, facilities, and current program of Mauna Loa Observatory in Hawaii, with emphasis on its suitability as a site for field studies on a wide variety of phenomena.

1. INTRODUCTION

The new high-altitude observatory established in July 1956 at an elevation of 11,150 feet on the slopes of Mauna Loa, in the Hawaiian Islands, has already been described by Fox [2,3]. The purpose of the present paper is to review the observatory's first 2 years and to consider in somewhat greater detail the climatic environment and such aspects of the physical setting, facilities, and programs most likely to interest those concerned with the possible suitability of such a mountain station for the study of specific phenomena within and outside the atmosphere.

Mauna Loa (Great Mountain) is situated on the island of Hawaii, largest and southernmost of the Hawaiian group (fig. 1). To the north it faces its sister peak, Mauna Kea, across a 6,000-foot saddle. To the east, west, and south it falls gently to the sea from its 13,680-foot summit, comprising thereby more than half the entire island (fig. 2). Measured from its roots on the ocean floor 18,000 feet below sea level, Mauna Loa is the earth's greatest single mountain mass. About 128 square miles of its surface lie above 10,000 feet.

Geologically, Hawaii is the youngest of the Hawaiian Islands. It is, in fact, still being formed [17]—a process to which Mauna Loa itself contributes by erupting every few years. Consequently, its slopes have not been eroded into the deep valleys and sharp ridges of the older, more northerly islands, but retain the smooth and gradual symmetry (the average grade is 7 percent) of the fresh volcanic cone (fig. 3). The lower slopes are regions of heavier rainfall and are densely vegetated; higher elevations are virtually barren wastes of dark lava.

At about 19°30′ N. latitude, Mauna Loa is well within the geographic Tropics. A solitary peak, except for Mauna Kea, and more than 2,000 miles from the nearest continental land mass, it lies in the midst of a tropical ocean which, in that vicinity, has a mean annual temperature of 75° F., an annual range of 5° F., and a daily range of less than 2° F.

The prevailing surface wind in this locality, south and west of the eastern Pacific high pressure cell, is the northeasterly trade, which has a frequency of 90 percent in summer and 80 percent for the year as a whole. Also characteristic of the region, and occurring with nearly the same frequency, is the trade inversion, whose average height of approximately 6,500 feet is only half that of Mauna Loa itself and corresponds to the mean timberline on its slopes.

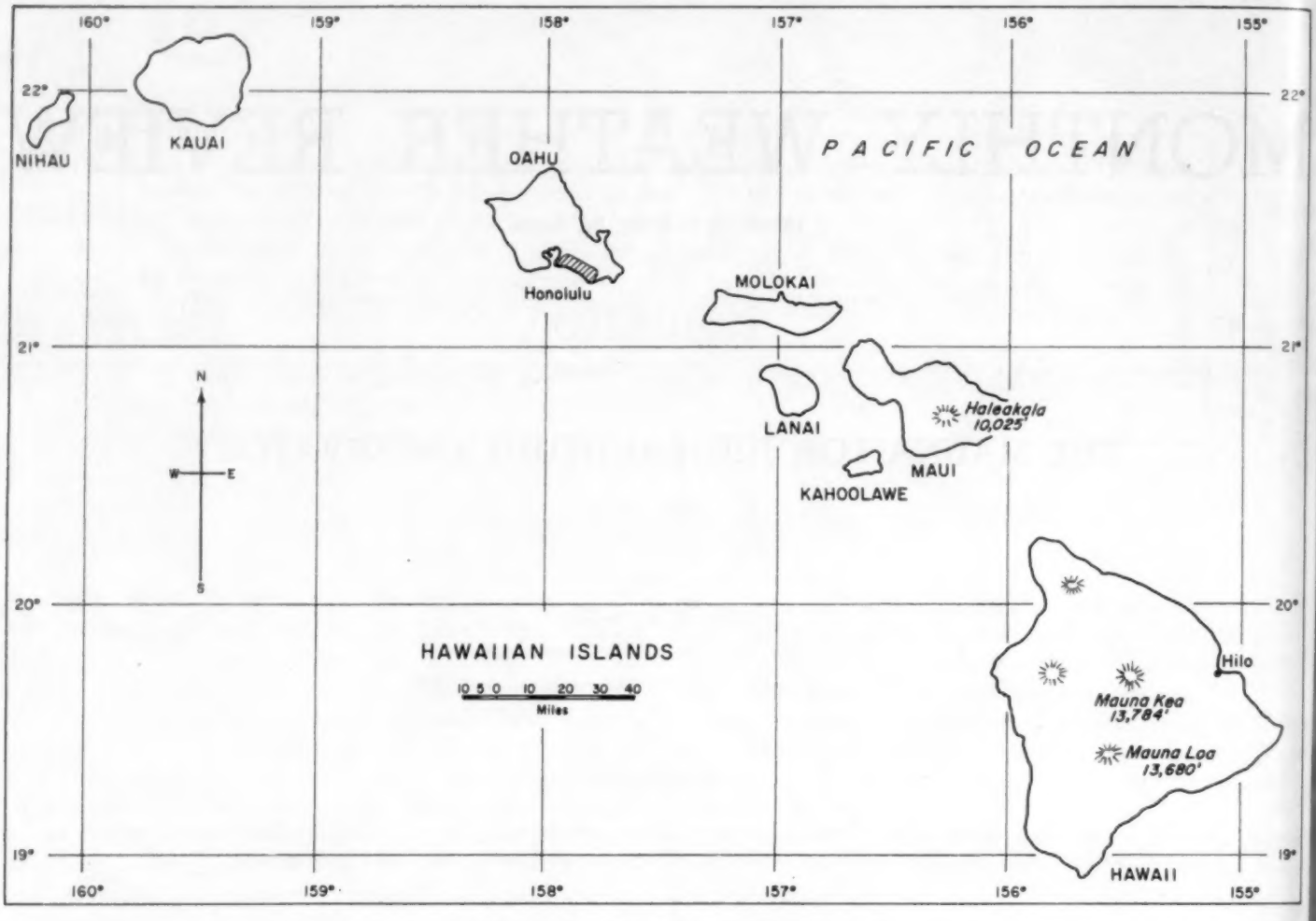

FIGURE 1.—The Hawaiian Islands.

2. HISTORY

The potential value of a high-altitude geophysical observatory in the oceanic Tropics had long been realized. The uniqueness of Mauna Loa in this respect—conferred by its height, insularity, mildness of climate at all elevations, distance from sources of industrial pollution, yet accessibility from large cities, freedom (due to the trade inversion) from most of the water vapor and debris of the lower atmosphere, and by the climatic uniformity of the maritime tropical environment—was given early recognition by the First Pan Pacific Science Congress which, meeting in Honolulu in 1921, adopted a resolution calling for the establishment of a weather station at the summit. But it was not until 1950 that the laying down across the lava wastes of a cinder road traversable by motor vehicles made the upper reaches of the mountain readily accessible and an observing station there feasible.

In December 1951, a small masonry hut was constructed at an elevation of 13,400 feet—one-fourth mile from, and 280 feet below, the summit. This was designed to house 90-day weight-driven recorders for atmospheric pressure, temperature, relative humidity, wind, sunshine, and precipitation, and to provide temporary shelter for scientific parties (fig. 4). Building and equipment were admittedly crude, and were regarded only as a first step toward the realization of a manned mountain observatory.

At the same time, rain gages and instrument shelters containing conventional barographs, hygrothermographs, and thermometers were placed along the slope at elevations of 5,100, 8,300, and 11,500 feet and, together with the summit station, were visited at intervals by employees of the U.S. Weather Bureau Office at Hilo, Hawaii. From the accumulating records, the first quantitative portrait of the climate of the upper mountain began to emerge [12].

In June 1956, in cooperation with the National Bureau of Standards, the Weather Bureau erected at 11,150 feet a much larger structure intended to provide working facilities and living quarters for extended stays by scientific parties or for a permanent staff. This was named the Slope Unit of the Mauna Loa Observatory, and will be referred to in what follows as the Mauna Loa Observatory or simply as the Observatory. With the assignment to Mauna Loa of an important role in the International Geophysical Year (IGY) [4] a permanent staff

of three Weather Bureau employees was appointed in July 1957 to conduct its programs of meteorological and other geophysical observations.

3. OBSERVATORY SITE

Altitude: 11,150 feet (3,398 meters)
Latitude: 19°32′ N.
Longitude: 155°35′ W.
Geomagnetic latitude: 19.9° N.

The Observatory lies within a leveled 4.05-acre plot on the gently sloping north-northeast face of Mauna Loa. On every side stretches the vast barren sea of dark aa lava,[1] loosely heaped and crumbling, which composes the mantle of the upper mountain, with here and there smaller patches of pahoehoe,[1] like pools of congealed molasses (fig. 5).

4. ACCESSIBILITY

From Hilo, the largest city (population 25,000) on the island of Hawaii, the Observatory is a 2-hour drive over 45 miles of crushed lava road. Honolulu, a modern American city of 300,000 and the cultural, economic, and population center of the Hawaiian Islands, with research institutes, technical libraries, and a large university, is only an hour and a quarter distant by air, with frequent daily commercial flights.

[1] The Hawaiian terms for the local lavas have entered into the vocabulary of volcanology. Aa resembles loosely strewn rubble; pahoehoe is billowy or ropy and, because it is often relatively unbroken, much more highly reflective than aa. Both are basic and have the same composition in the molten state. Differences arise during cooling, the aa forming at lower temperatures, smaller gas content, and more advanced crystallization. See Gordon A. MacDonald, "Pahoehoe, Aa, and Block Lava," *American Journal of Science*, vol. 251, Mar. 1951, pp. 169-191.

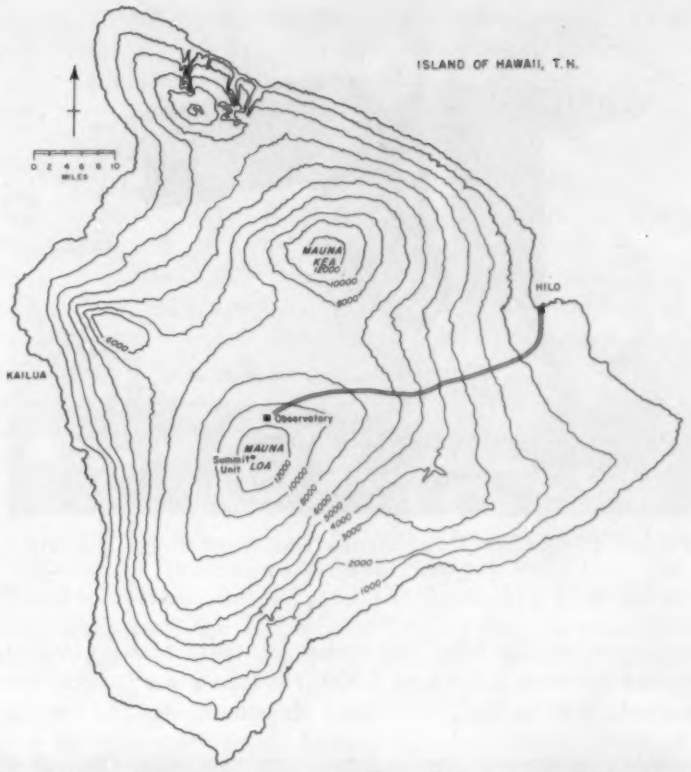

FIGURE 2.—Topographic map of Hawaii showing the Slope and Summit Units of the Mauna Loa Observatory, and the road from Hilo.

The road up Mauna Loa gradually ascends the northeast face of the mountain, through a luxuriant tropical rain forest of epiphyte-covered trees, ferns, and sedge flourishing upon the lava. Along the route the average rainfall

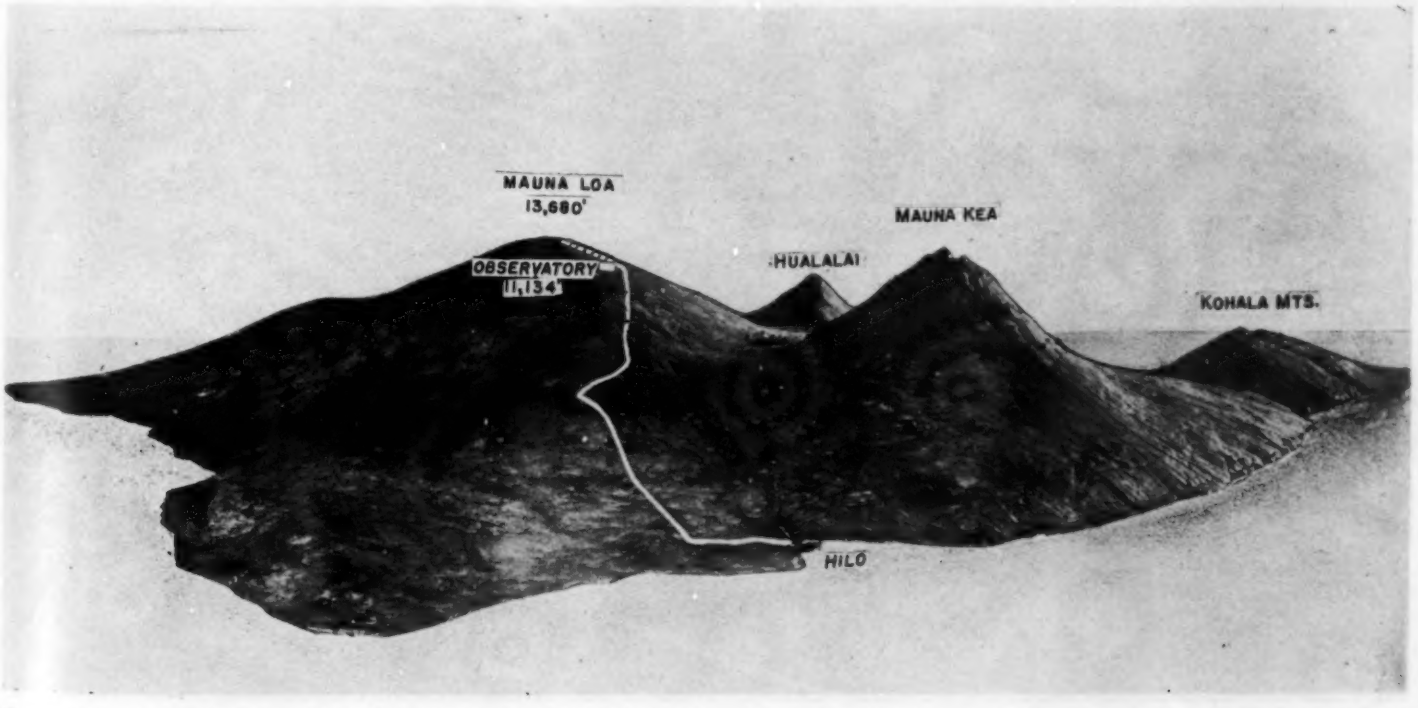

FIGURE 3.—Hawaii, photographed from a model at the University of Hawaii, and showing the smooth slopes, gentle gradients, and symmetry of Mauna Loa. Vertical exaggeration, 2.5 times.

FIGURE 4.—Summit Unit, Mauna Loa Observatory. Elevation 13,400 feet (4,084 meters).

increases rapidly from 145 inches annually at Hilo to 250 inches between 2,500 and 3,000 feet (the island maximum exceeds 300 inches) and then decreases steadily to an estimated 15 inches at the summit. At about 6,000 feet the forest opens abruptly into fields of aa dotted with shrubs and scattered stands of trees. Soon these too grow sparse, and the road continues over a lava expanse broken only by gray patches of moss and lichens and an occasional shrub.

The road is maintained as a public highway by the Territory of Hawaii only to near the 6,000-foot level. Above that point, deterioration of the unconsolidated surface by weather and use presents a continuing problem, and a good paved road to the Observatory, and eventually to the summit itself, remains Mauna Loa's greatest present need. Still, except for short stretches where some difficulty in traction over the loose, hilly surface might be encountered, the road to the Observatory is negotiable by passenger car, with due caution against overheating and, possibly, carburetor adjustment with increasing altitude. However, a 4-wheel drive is preferable and, for the additional 8 miles to the summit, essential. For its own needs, the Observatory maintains two 4-wheel drive vehicles, one an open truck, the other an enclosed carryall. These make several round trips weekly and in rotation, leaving one vehicle always at the Observatory for emergency use.

FIGURE 5.—Aerial view of the Observatory, looking south (upslope), taken in bright sunlight. The very dark background is the aa lava which largely covers the upper mountain. Lighter patches are pahoehoe lava. The leveled 4.05-acre plot on which the Observatory stands is plainly visible. The road to the summit leads off to the right.

5. FACILITIES

The main building of the Observatory is a 20-by-40-foot concrete block structure, well insulated, and having a peaked roof of corrugated aluminum (fig. 6). It is partitioned internally into a comfortably furnished 16-by-20-foot living room-office (fig. 7), an instrument room, two bedrooms with accommodations for six, and a kitchen-dining room with propane hot water heater, cooking range, and refrigerator.

Along its south side is a concrete slab, 15 by 45 feet, for mounting instruments outdoors. Auxiliary structures include a wooden tower 8 by 8 feet with a platform 12.5 feet above the ground; the generator shed; the Dobson and various other instrument housings; fuel and water tanks; and the anemometer mast.

Electricity.—110-volt, single-phase, 60-cycle alternating current for household use and the scientific instruments is furnished by two recently installed 35 kw. diesel generators. These provide a more dependable source of electric power than that previously available, and are being operated alternately to permit preventive maintenance and thus insure against power interruptions. Since present use is approximately 10 kw., a substantial reserve remains to meet additional requirements. Three frequency regulators, with a total capacity of 600 watts, control the frequency to the more critical circuits and to the recorders.

Water is obtained by roof catchment drained into a 1,000-gallon tank and augmented, if necessary, by haulage from Hilo.

Workshop space is provided in the generator shed and in the enclosed base of the wooden tower. The Observatory is equipped with a small, but well-chosen, technical library, two desk calculators for data reduction, a microscope, the usual hand tools, a drill press, and a variety of electrical and electronic test instruments. Additional facilities for the purchase, fabrication, and repair of equipment are to be had in Hilo and Honolulu.

Communications.—50-watt transceivers at Mauna Loa maintain an open 24-hour radio contact with the Hilo Weather Bureau station, and the feasibility of a direct radio link with the Honolulu office, as well, is presently being explored. Mobile units identical to those at the

FIGURE 6.—The Mauna Loa Observatory, looking north. From left to right: (1) generator shed, (2) solar radiation instruments, (3) rain gages and instrument shelter, (4) diesel fuel tank, (5) anemometer mast, (6) water tank, (7) main building, (8) concrete apron, (9) Kiess-Corliss spectrograph shelter (see reference [6]), (10) Dobson spectrophotometer housing, (11) instrument platform, (12) fission products collector. In the background is Mauna Kea, about 25 miles distant. Intervening clouds are trade wind cumuli and lie over the saddle and below the level of the Observatory.

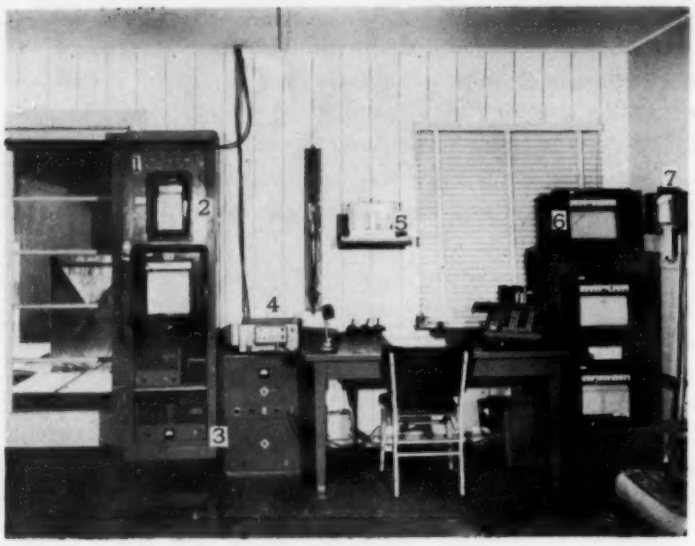

FIGURE 7.—Interior view of the Observatory's living room-office, south wall. (1) sunshine panel; (2) wind, sunshine, rainfall recorders; (3) frequency regulators; (4) 50-watt transceiver; (5) microbarograph; (6) from top to bottom, recorders for horizontal and normal incidence pyrheliometers, radiometer temperatures, and net exchange and total hemispherical radiometers; (7) recorder for surface ozone.

Observatory are mounted also in its vehicles. A powerful AM-FM-short wave receiver and a television set contribute to the recreation of staff and visitors. Reception is excellent.

6. STAFF

The Observatory's present complement includes the physicist-in-charge, two meteorological aides, and an electronics technician. Except for the latter, staff members spend 6 successive days on Mauna Loa and the seventh in Hilo, where those who are married maintain family residences. At least two persons remain on duty at the Observatory at any time. The principal responsibilities of the staff are to operate and service the scientific instruments, to take hourly weather observations, to reduce portions of the data, to cooperate in the projects of visiting scientists, and to do research.

Although visitors do occasionally experience some of the well-known discomforts of mountain sickness, the staff's acclimatization to the altitude has been complete and their general level of health excellent.

7. CLIMATE AND WEATHER

Unfortunately for so rich a subject, the scope of the present paper precludes more than a few remarks and some illustrative data concerning the weather and climate of the Observatory site. Additional information on the various and diverse climatic regimes of Mauna Loa, including its summit, is available in [12]. A fuller account is in preparation.

As might be anticipated from the tropical maritime locale, the Observatory's climate is comparatively mild for the altitude. Severe or violent weather is infrequent and the rigors of life at Alpine stations virtually unknown. On the contrary, the brilliant skies and intense insolation, the moderate temperature and low humidity, experienced in so bizarre and remote a setting, induce in most visitors feelings of exhilaration and well-being.

The Mountain circulation.—Like other mountains, Mauna Loa imposes upon the surrounding atmosphere a local circulation often remarkably indifferent to the large-scale movement of air in the region. This circulation has a complex origin, being due in part to mechanical interference by the mountain with the otherwise free flow of air in its vicinity, in part to differential heating and cooling of its slopes relative to one another and to the free air, and in part to pressure gradients set up by temperature differences at similar altitudes between the atmospheric strata overlying the mountain and those more distant. The thermally induced components in this motion resemble an immense respiration—inward and upslope during the day, downslope and outward at night—which is reflected in characteristic diurnal variations in the weather. The wind shifts from night to day, and humidity, cloudiness, rainfall frequency, and turbidity tend to increase toward afternoon with the influx of air from lower elevations.

Thus, a typical day at the Observatory may dawn bright and clear. Visibility is excellent. Peaks on other islands 80 miles distant and more are distinguishable without difficulty. The trade inversion lies several thousand feet below, and trapped beneath it are the clouds and the bulk of the water vapor, dust, and haze. In the clear atmosphere insolation is intense—frequently over 1.70 cal. $cm.^{-2}$ $min.^{-1}$ at true solar noon—and the temperature of the black lava and of the air rises rapidly.

By early afternoon, moister air appears to be seeping upward along the mountain. The humidity increases and fractocumuli advance up the slopes. In the next hours the Observatory may be briefly enveloped in fog or light rain; but by evening the clouds have dissipated and the conditions which opened the day return. Nights are generally clear. Of course, individual days may vary widely from this regime.

The role of the trade inversion in this process is not completely understood. Almost unquestionably it may impede, but does not necessarily prevent, vertical transport of air along the slopes; so that on Mauna Loa, as on mountains elsewhere, the local circulation dominates the diurnal aspects of climate.

Through turbulent exchange, mountains tend also to take on the properties of the surrounding free air. This is more pronounced at summits (because of their greater exposure) than on the slopes and for seasonal than for diurnal factors.

Thus the climate at the Observatory reflects the influences of the mountain circulation, the free air, the continentality of Mauna Loa's own great bulk and surface area, and the tropical maritime surroundings. The data which follow combine the year-long record at the Observatory with the temperature, humidity, and rainfall for

TABLE 1.—*Temperature (° F.) at or near Mauna Loa Observatory*

	Jan.	Feb.	Mar.	Apr.	May	June	July	Aug.	Sept.	Oct.	Nov.	Dec.
Highest of record	62	63	60	65	68	70	70	69	67	68	64	67
Mean maximum	48.4	46.6	49.3	53.6	55.8	58.8	58.7	58.6	57.8	56.5	53.0	49.6
Mean minimum	29.6	28.9	31.3	33.7	34.5	37.1	35.6	36.6	36.7	36.6	33.3	31.9
Lowest of record	22	20	20	25	24	24	26	29	29	29	23	22
Mean daily range	18.8	17.7	18.0	19.9	21.3	21.7	21.1	20.0	21.1	19.9	19.7	17.7
Years of record	6	5	4	6	6	6	6	5	5	5	5	5

several earlier years at two nearby stations, first at 11,500 feet and later at 10,958 feet.

Temperature.—The mean monthly maximum and minimum temperatures, the mean daily range, the highest and lowest observed, and the years of record are given in table 1. Although a detailed commentary cannot be undertaken here, the moderateness, even of the extremes, is noteworthy. The rapid rise of temperature in the spring, its more gradual decline in autumn, and the early maximum with a second peak in late summer, are all predominantly marine and free air in character. The diurnal range, on the other hand—large for the altitude and the oceanic Tropics—is attributable to the great expanse of the upper mountain and to the radiative properties of its dark lavas.

Rainfall.—The chief year-round source of rainfall in the Hawaiian Islands is orographic uplift of the moist trade wind. During the cooler season, and in the absence of the trade, this is complemented by rainfall associated with frontal passages and cyclonic circulations, including the so-called Kona storms, and in the island interiors and uplands by convective showers.

Observations made over a 4-year period at or near the Observatory are summarized in table 2A.

The mean annual rainfall of approximately 25 inches appears to be consistent with extrapolations from island-wide isohyetal charts based on longer periods of record, but using only gages below about 6,000 feet.

The record is much too short to justify reading a seasonal trend into it, but the intimation of a double maximum is at least not incompatible with the cyclonic rainfall contribution of winter and the greater frequency during the summer of local convective showers on the upper mountain. The wettest month of record was January 1956 with 12.89 inches. The variability of rainfall is suggested by the fact that in 1958 the same month had only a trace.

The indication in table 2B of a maximum frequency in late afternoon presumably reflects again the formation of showers within the ascending mountain currents, and is in contrast with the nocturnal maximum characteristic of a marine climate and found at lower elevations in regions exposed to the trades.

Wind.—Continuous observations of wind at the Observatory site date only from July 1957, but appear to confirm others made during short intervals over the preceding years. On the whole, speeds are moderate, and no obvious topographic accelerations have been evident. Strongest winds of the year were the sustained speeds of 75 m.p.h. with gusts to 100 experienced in March 1958. This was not, however, a local condition, but a time of high wind generally, due to an unusual situation—the proximity of a tropical storm. Again in January 1959 a similar event occurred, this time producing average winds of 80 m.p.h. with gusts exceeding 105.

Table 3 shows for January and July 1958 the average hourly speed and the frequencies of specified directions. July winds, in the mean, slightly exceeded those for January, but evidence of seasonality from so brief a record is questionable. On the other hand, the abrupt turnabout from southerly (downslope) flow at night to the upslope directions (west through north to east) during the day is unmistakable, and—as was mentioned earlier—is in marked contrast with the winds in the nearby free air, which exhibit little diurnal variation. The reversals in air movement, being related to the heating and cooling of the mountain slopes, follow shortly after sunrise and sunset (compare, in this respect, January with July); the lightest wind occurs at the times of the reversals.

Humidity.—With the bulk of water vapor confined by the trade inversion to levels below the Observatory for most of the day, the average absolute humidity is low. The relative humidity displays two noteworthy characteristics: first, a diurnal course quite unlike that commonly observed, in that humidity on many days tends to vary directly, rather than inversely, with temperature (fig. 8); and second, a high frequency of exceptionally low humidities—often below 5 percent for extended periods, and occasionally below 1 percent for most of a day. The first proceeds directly from the invasion of the upper slopes by lower level air during the afternoon. The second is more obscure, being at times almost certainly

TABLE 2.—*Precipitation at Mauna Loa Observatory*

A. Mean Monthly Rainfall		B. Hourly Rainfall, Percentage Frequency (trace or more) of All Observations			
Month	Inches	Hour ending (LST)	%	Hour ending (LST)	%
January	3.9	01	2.0	13	4.9
February	2.1	02	2.6	14	6.6
March	4.0	03	2.0	15	6.1
April	0.7	04	2.0	16	6.4
May	1.2	05	2.3	17	7.5
June	0.3	06	2.6	18	6.4
July	2.0	07	2.6	19	4.0
August	2.9	08	2.9	20	4.0
September	1.9	09	2.3	21	2.6
October	1.2	10	3.2	22	1.7
November	1.5	11	3.5	23	1.7
December	3.4	12	4.0	24	2.3

498746—59——2

TABLE 3.—*Mean hourly winds at Mauna Loa Observatory*

January 1958, Monthly Mean 9.1 m.p.h.

Hour ending (LST)	01	02	03	04	05	06	* 07	08	09	10	11	12	13	14	15	16	17	* 18	19	20	21	22	23	24
Percentage W through E	19	13	16	13	16	16	16	16	19	71	90	100	100	100	100	100	94	74	61	42	19	16	13	16
Percentage SE through SW	81	87	84	87	84	84	84	84	77	26	10	0	0	0	0	0	6	23	29	58	81	84	87	84
Mean wind speed (m.p.h.)	9.4	9.4	9.6	9.8	10.7	10.3	9.9	9.8	7.0	5.5	7.1	7.6	9.5	10.1	10.2	9.6	8.9	7.6	6.9	8.2	9.2	9.5	10.2	10.6

July 1958, Monthly Mean 9.5 m.p.h.

Hour ending (LST)	01	02	03	04	05	* 06	07	08	09	10	11	12	13	14	15	16	17	18	* 19	20	21	22	23	24
Percentage W through E	0	0	0	0	0	0	0	39	81	84	94	90	90	97	97	97	100	94	90	48	10	6	6	3
Percentage SE through SW	97	97	97	100	94	100	100	52	19	16	6	10	3	3	3	3	0	6	6	45	81	94	90	97
Mean wind speed (m.p.h.)	11.5	10.6	10.8	10.3	10.5	10.1	9.4	7.1	7.3	8.3	9.4	10.5	11.0	10.8	10.6	9.9	9.4	8.5	7.7	6.4	7.3	9.3	10.2	10.3

*Indicates sunrise and sunset.
Underscore indicates minimum wind speed.
Double underscore indicates maximum wind speed.

due to nocturnal subsidence over the radiatively cooled mountain, but at other times—as when low humidity persists through the day—to the breaking down of the ascending mountain current (perhaps when insolation is weak and the inversion strong), or to marked subsidence within the general air flow around the southern flank of the Pacific High.

Measurements of the total precipitable water above Mauna Loa [16] suggest that the afternoon rise in surface humidity involves only a relatively thin skin of moister air.

Clouds and sunshine.—Visual observations, from which the diurnal and seasonal variations in cloud types and frequencies could be obtained, are available only for a portion of the daylight hours and the single year that the Observatory has been manned. Other useful indices of sky cover are the proportion of possible sunshine received in each daylight hour and the frequency of clear, partially obscured, and overcast skies. Observations of the latter kind are summarized in table 4 for August 1957 through February 1958.

Since even the thinnest and most transparent clouds were included in this tabulation, it considerably understates the sunniness of the site and the frequency with which the solar disc can be seen; and it would appear from these and other data that about 90 percent of the nighttime and well over 50 percent of the daytime hours are nearly or entirely free from cloud above the level of the Observatory.

The afternoon maximum in sky cover is due again primarily to the formation of fractocumuli in air rising along the mountain slopes. Perhaps because of its smooth terrain and gentle slope, Mauna Loa has fewer orogenic cirrus than do some of the lower but more abrupt mountain barriers of the other islands.

TABLE 4.—*Mean hourly sky cover (percentage frequency) at Mauna Loa Observatory*

Hour of observation (LST)	08	09	10	11	12	13	14	15	16	17
Clear skies	59	56	52	47	38	29	21	18	19	24
Half-covered sky or less	74	71	70	66	59	49	37	37	38	46
Overcast	16	14	17	23	20	28	31	35	31	25

Snow.—Although it has on the average several snowfalls each winter, Mauna Loa does not even then bear a permanent snow mantle. Snow, usually light, also occurs at the Observatory from time to time, but the mean snow line is at about 12,000 feet. With intense insolation and low humidity, evaporation is extremely rapid; yet snow has been found at the summit even in midsummer, tucked away beneath the lava.

Thunder, lightning, hail.—Like other severe weather, these are infrequent and relatively mild at the Observatory. From July 1957 to August 1958 only 5 days had thunderstorms, and on all these occasions hail approximately one-sixteenth inch in diameter was also observed.

"Seeing" and turbidity.—Visiting astronomers [6] have found the "seeing" highly satisfactory, but systematic observations of it, day and night, have not yet been attempted. However, computations of turbidity from solar radiation measurements (q.v.) will soon begin. Scattering in the circumsolar region appears to be minimal.

8. SOME SCIENTIFIC USES

IN THE PAST

In the 2 years since the construction of the Observatory, a number of scientific endeavors have taken advantage of its elevation, the low turbidity and water vapor content of the overlying atmosphere, or some other special attribute of the site. These studies are briefly listed below, with references to published reports wherever possible.

The forms taken by snow crystals growing under natural conditions in an aerosol-free environment, December 1956 to January 1957, Geophysical Research Directorate [9]. With the buildings at 11,150 feet providing a base of operations, microphotographs were taken of freshly fallen snow flakes at the summit of Mauna Loa.

Spectrographic observations of water vapor in the atmosphere of Mars during that planet's close approach in July 1956 and of Jupiter in May 1957, National Geo-

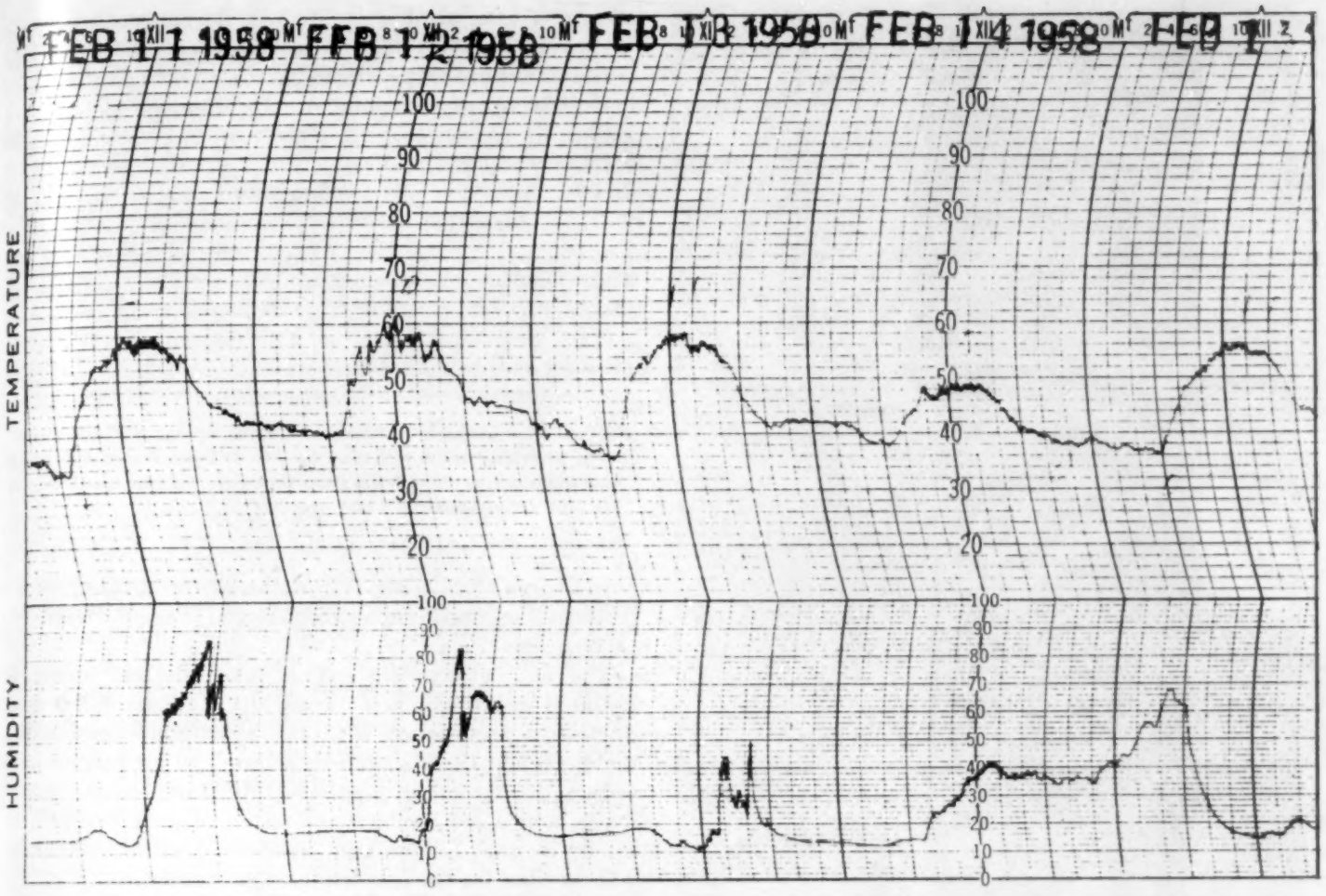

FIGURE 8.—A representative hygrothermograph chart, Mauna Loa Observatory. The tendency for humidity to increase during the afternoon probably reflects the influx of air from lower levels.

graphic Society and National Bureau of Standards [6]. A high-dispersion laboratory-type instrument was used. The prime requisite was a minimum of water vapor in the terrestrial atmosphere.

Spectroradiometry of the sun between 0.3 and 2.5 microns, June 1956 and May 1957, National Bureau of Standards [16]. A lead sulfide cell and a photoemission tube were used in these observations to cover the spectral range. Strong absorption by water vapor in this band required that the superambient atmosphere be as free from it as possible.

Atmospheric transmission in the infrared, July to September 1957, Naval Research Laboratory [19]. Light from two 5-foot carbon-arc searchlights mounted at about 10,000 feet on the facing (south) slope of Mauna Kea was analyzed by an infrared spectrometer at the Observatory, 17 miles distant. This project utilized the long optical path through the clear air above the inversion offered by the facing sister peaks (fig. 2).

Lunar occultation program, October 1957, Army Map Service. Precision timing of stellar occultations by a photo-multiplier operating off a 12-inch reflecting telescope was used to connect the Hawaiian Islands with the North American geodetic datum.

PRESENT PROGRAMS

Present observations at Mauna Loa are of three kinds: local weather; continuation of the International Geophysical Year (IGY) programs in atmospheric composition, solar radiation, and particulate matter; and others for special purposes. Pertinent meteorological observations and synoptic analyses are made also at Hilo and Honolulu.[2]

Routine meteorological observations and analyses.—At the Observatory, local weather is recorded hourly between 0600 and 1700 LST and autographic tracings are obtained of the atmospheric pressure, temperature, relative humidity, wind speed and direction, precipitation, and duration of sunshine. Time-lapse cloud photography is used routinely to preserve the visual aspect of the weather.

These observations serve not only the usual meteorological and climatological purposes, but by describing the local state of the atmosphere they provide the correlative information needed to validate and interpret data from the IGY and other programs. An example of this is the present attempt by the authors to account for the diurnal

[2] Programs in geomagnetism, solar flares, and cosmic rays begun during the IGY are in progress elsewhere in the Hawaiian Islands, including the 10,000-foot summit of Haleakala, Maui, by the University of Hawaii and other organizations.

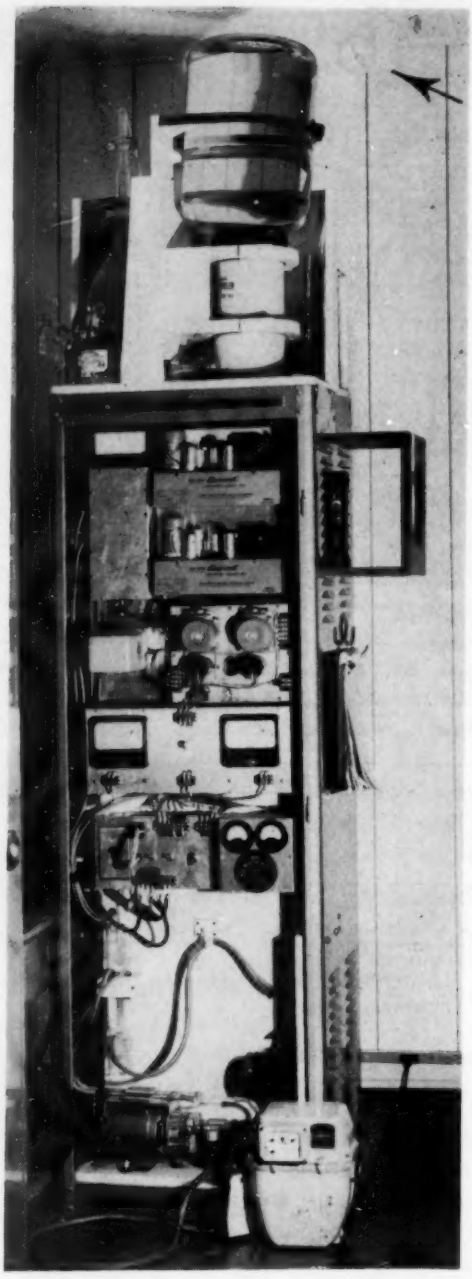

FIGURE 9.—Regener automatic surface ozone recorder. Arrow points to glass tubing from air intake mounted 3 feet above the Observatory roof.

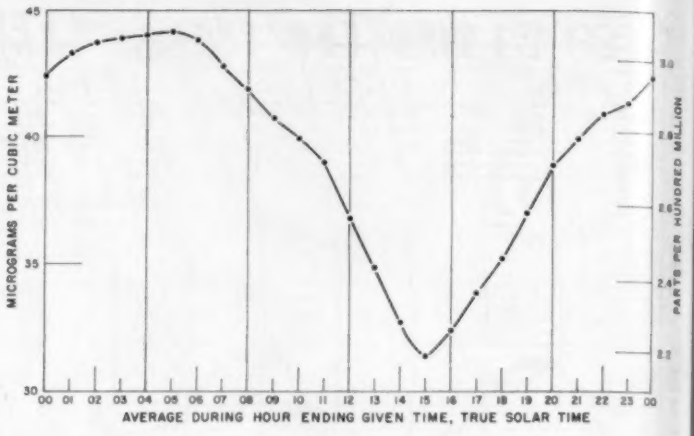

FIGURE 10.—Diurnal variation of surface ozone, November 1957. The afternoon minimum may be due to the influx of lower-level air whose ozone content has been depleted by contact with vegetation or aerosol-bearing water droplets.

variation in surface ozone at Mauna Loa in terms of the mountain circulation.

Further correlative information is provided by the Weather Bureau's aerological station at Hilo where upper-air soundings of temperature, humidity, and wind, often to altitudes of 30 km., are made twice daily (at 0200 and 1400 LST, four times daily on IGY World Days), and by the extensive analysis and forecasting program of the Honolulu Weather Bureau Airport Station, 210 miles to the northwest, which prepares synoptic charts of the broadscale circulation of the atmosphere at sea level (4 times daily) and at 700, 500, and 300 mb. (twice daily) over an area which extends from the western United States, through the northern and equatorial Pacific Ocean, to eastern Asia.

The IGY observations.—The meteorological programs initiated at Mauna Loa during the IGY are being conducted in accordance with the appropriate instruction manuals, and these should be referred to for further procedural details concerning them [15]. Instruments, procedures, and a few preliminary results will be touched on briefly in what follows and, wherever possible, references will be cited for the less familiar observations.

Surface ozone.—Continuous recordings of surface ozone have been made since August 1957 by means of automatic chemical sampling equipment recently developed by Regener [14]. The procedure, which is absolute and highly specific for ozone, utilizes the differential oxidation of potassium iodide to iodine within two air streams, one of them heated to 300° C. to dissociate its ozone. Sodium thiosulphate is used to prevent volatilization of the iodine. The resolving time of the instrument is approximately one minute.

A preliminary study of the first 14 months of record indicates that the variations in surface ozone at Mauna Loa are related to both local and large-scale features of the atmospheric circulation. A marked seasonality is evident, with a spring maximum and autumn minimum like that found elsewhere in surface and total ozone. Monthly means ranged from 33 micrograms per cubic meter in October 1957 to 68 micrograms per cubic meter in April 1958, the rise being especially steep from late winter to early spring. The lowest mean hourly value observed was about 20 and the highest near 100 micrograms per cubic meter; the lowest and highest 1-minute values were approximately 7 and 135 micrograms per cubic meter, respectively.

Superimposed upon these seasonal trends, and often of comparable amplitude, is a pronounced diurnal variation with early morning maxima (a secondary peak is common

shortly after sunrise) and minima during midafternoon (fig. 10). This is attributed to the local circulation of up- and down-slope winds generated by the radiational heating and cooling of the mountain itself, the afternoon minimum being more specifically ascribed to the influx from below of air whose ozone content has been depleted during its ascent by contact with vegetation, water droplets, or aerosols in the moist subinversion layer (below about 6,500 feet).

Striking variations in the amount of surface ozone have also been observed to accompany changes in the broad circulation patterns in the Pacific area. Thus, during February 1958 ozone increased abruptly with the transition from the prevailing trade wind regime to a strong westerly flow around deep cyclones centered some distance north of the Hawaiian Islands, and decreased again with the return of the trades. A report on these observations is in preparation.

Total ozone.—The Observatory's Dobson Spectrophotometer (No. 63), by which the total depth of atmospheric ozone is determined from the differential absorption by ozone of two spectral lines in the ultraviolet portion of the solar beam, was put into operation on November 27, 1957. Its elevation (it is the highest permanent installation of its kind), the clarity of the overlying atmosphere, and the relatively small ozone variations typical of the latitude are expected to make its observations valuable not only for their contribution to the synoptic ozone program, but also for calibration purposes—principally the determination of the extraterrestrial constants. The Mauna Loa spectrophotometer is to be used as a standard for the United States Dobson network.

Lunar observations from 3 days before to 3 days after full moon are also being made, and these will be compared with those in the Antarctic where changes in the moon's angular elevation are too small for close calibration of the instrument.

On the basis of the first 10 months of record, day-to-day variations in total ozone at Mauna Loa appear to be small, but the amounts themselves and the amplitude of the seasonal variation, which ranged from approximately .250 cm. in February to .288 cm. in May 1958 (the Vigroux absorption coefficients were used in these computations) are high for the latitude [13]. However, these values and the late occurrence of the seasonal peak relative to that in middle and high latitudes must await the confirmation of additional observations.

Carbon dioxide.—As part of the worldwide effort begun during the IGY to obtain baseline measurements suitable for defining the present CO_2 content of the atmosphere and thus detect secular trends, this component is being continuously recorded at Mauna Loa Observatory by means of a Model 70 Infrared Gas Analyzer (fig. 11), an instrument specifically designed for the monitoring of flowing gas samples [1].

The analyzer operates by measuring the energy loss

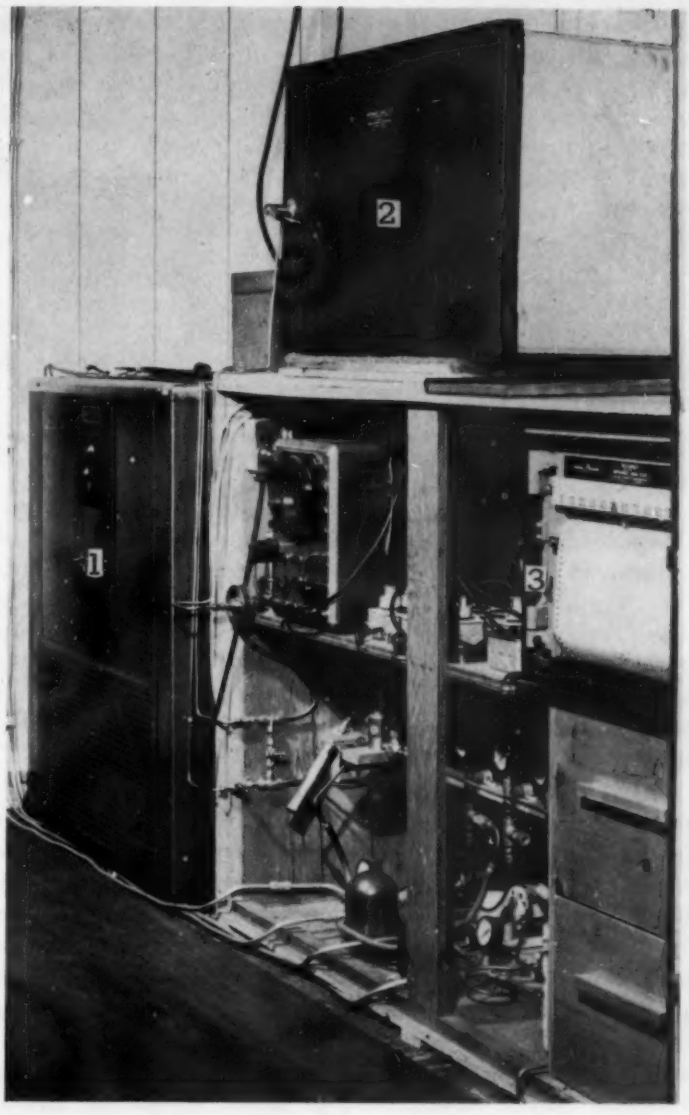

FIGURE 11.—Infrared analyzer for CO_2. (1) freezer to remove water vapor which would otherwise interfere with the analysis, (2) analyzer box, (3) recorder.

of an infrared beam traversing a gas sample. Radiation from an infrared source, after being mechanically chopped at 20 c.p.s., passes through the test-gas-filled cell, where its absorption produces a cyclic pressure pulsation. This is transmitted to the tantalum diaphragm of a condenser microphone and thence converted to a voltage which is recorded. A reference gas of known CO_2 content is used as a standard. Air intakes are mounted on four 20-foot towers 450 to 500 feet distant and in mutually perpendicular directions from the main Observatory buildings. Two upwind flows are sampled concurrently, any difference between them being interpreted as due to local contamination.

Data secured at Mauna Loa since sampling began in March 1958 are sufficiently similar to those obtained elsewhere to support previous indications that in the absence of local pollution the carbon dioxide concentration in the lower atmosphere is substantially uniform over the earth.

FIGURE 12.—Solar radiation instruments, facing northeast. From left to right, Beckman and Whitley (Gier and Dunkle) total hemispherical and net exchange radiometers, and Eppley normal incidence and horizontal incidence pyrheliometers. Notice the loose, rough texture of the ground.

The Observatory data also suggest a diurnal variation, perhaps related again to the mountain circulation, and a seasonal trend, with mean monthly values decreasing gradually from approximately 314 p.p.m. (parts per million) in May to 312 p.p.m. in August.

Solar radiation.—The solar radiation measurements made at Mauna Loa since November 1957 are part of an international program designed to increase our knowledge of the radiation fluxes to and from the earth's surface, and hence of the earth's heat balance and budget. The instruments being employed for this purpose at Mauna Loa are shown in figure 12. They include the Eppley (10-junction) horizontal incidence pyrheliometer (pyranometer) for the total incoming (short wave) radiation from sun and sky; the Eppley normal incidence pyrheliometer, for direct solar radiation (solar intensity), equatorially mounted and driven by a synchronous motor to follow the sun; the Beckman and Whitley (Gier and Dunkle) total hemispherical radiometer for the total (long wave, terrestrial) radiation from earth and atmosphere; and the Beckman and Whitley net exchange radiometer for the net transfer of (long wave) radiation between earth and atmosphere ([15 Part VI], [5]). All are continuously recording.

Filters (Nos. OG1, RG2, and RG8) for subdividing the spectral regions are to be used with the normal incidence pyrheliometer, thus—among other things—permitting the turbidity coefficients to be computed.

Fission products.—The use of the radioactive products of nuclear tests as tracer materials for studying the atmospheric circulation has been described by Machta [8]. As one of the network of fallout stations, Mauna Loa has operated, since August 1957, a small (40 c.f.m.) air filtration system in which a week's run constitutes a single sample. Filters are sent for analysis to the Naval Research Laboratory, Washington, D.C.

Freezing nuclei.—The Bigg-Warner expansion chamber

FIGURE 13.—Bigg-Warner expansion chamber for measuring the concentration of freezing nuclei.

developed by the Australian Commonwealth Scientific and Industrial Research Organization for measuring the concentration of freezing nuclei [18] is shown in figure 13. Freezing nuclei in the refrigerated air sample trigger the formation of ice crystals in the fog produced on expansion. These crystals fall into a dish of slightly supercooled sugar solution at the bottom of the 10-liter tank, where they enlarge rapidly and may be readily counted by inspection. By varying the initial overpressure to which the air sample is subjected, a spectrum of the freezing nuclei population as a function of temperature may be obtained.

Daily counts made at the Observatory since December 1957 show preliminary evidence of occasional peaks occurring within a few days of those observed elsewhere. A current hypothesis in the field relates anomalous freezing nuclei activity to meteor showers a month earlier and to singularities in rainfall, cirrus cloudiness, and other geophysical phenomena. The Mauna Loa data are included in a recent summary by Kline and Brier [7] of these apparent correlations.

Micrometeorites.—The scavenging of cosmic dust from large volumes of air pumped through fibreglass filters began at Mauna Loa in August 1957 at the request of the Swedish oceanographer, Hans Pettersson, who saw in the deposition rate of micrometeoritic materials on the earth's surface a possible means of dating the oceanic sediments [10]. After a weekly 24-hour run, the filters are analyzed for iron, nickel, and cobalt in the II Chemisches Institut der Universität, Vienna. Nickel, believed far in excess of any possible contamination from terrestrial sources, has been found in most of the filters from Mauna Loa [11].

FOR THE FUTURE

The year since the assignment of a permanent staff to the Observatory has been occupied largely with the installation, calibration, and maintenance of the scientific equipment and, more recently, with the reduction of data for forwarding to IGY collection centers. Because of their value virtually all the IGY programs at Mauna Loa have been continued beyond the official termination of the International Geophysical Year in December 1958.

As the instrumental and observational aspects of the work settle into routine, a limited amount of time is also becoming available for a preliminary study and interpretation of the record and, on a modest scale, for additional investigations which reflect the personal interests of the staff.

Mountain circulation and climate.—The motions and properties of the lower 1,000 feet of Mauna Loa's atmospheric envelope, and the structure and role in the mountain circulation of the trade inversion contiguous to the slopes, are to be explored—at first by wiresonde profiles and soundings of temperature, humidity, and wind, and later by more elaborate means. In addition to their intrinsic interest and their pertinence to an evaluation of the local factors in Mauna Loa's weather and climate, it is hoped that these observations may permit the exchange coefficients within the mountain's envelope and between it and the surrounding air to be computed.

Atmospheric interrelationships.—The ready accessibility at the Observatory of the weather records on the one hand (local, upper air, synoptic charts) and the IGY observations on the other (ozone, carbon dioxide, solar radiation) makes it a convenient place in which to study the interrelationships between them; that is, the meteorological correlates of diurnal, seasonal, and synoptic variations in ozone, carbon dioxide, and radiation, and conversely, the possibility of anticipating synoptic developments—for example, the formation and motion of Kona storms—through precursory variations in, say, total ozone.

Others.—Among other projects now in prospect for Mauna Loa are observations of the vertical gradients of ozone (by ozonesonde) and carbon dioxide (by flask sampling and aircraft traverses) along the mountain slopes and in the nearby free air. More accurate determinations of surface humidity and of the total precipitable water in the overlying atmosphere await the receipt of stable infrared hygrometers. The local and synoptic concomitants of the exceptionally low humidities commented upon earlier are also to be looked into. The freedom of the site from the pollution almost invariably present in continental air masses makes it well suited to baseline observations of atmospheric electricity, and measurements of conductivity, potential gradient, and ionization rate are being planned.

These and other proposed studies must, of course, be contingent on the availability of suitable instruments and on prior obligations to the IGY and other present programs.

9. CONCLUSION

The elevation and accessibility of the Mauna Loa Observatory, the comfort in which high-altitude work can be done throughout the year, its insularity, and its isolation during the night and much of the day from a large part of the tropospheric water vapor and turbidity, are advantageous for many observations within and outside the atmosphere. It is especially suited for those which require exceptional transparency of the air, and has already been utilized in a number of such projects.

The usefulness of the Observatory, particularly for the determination of standard or baseline values of, and secular trends in, solar radiation, the atmospheric constituents, and for other observations is further enhanced by its geographical isolation. Scarcely the slightest prospect exists that within the foreseeable future the site can deteriorate significantly through the encroachment of cities or industry upon the present highly stable population and specialized agricultural economy.

A good paved road and, less immediately, commercial electric power remain the Observatory's most pressing needs. However, increasing recognition that the present site at 11,150 feet and the summit 2,500 feet above are potentially among the world's most valuable terrestrial platforms, leaves little doubt that these improvements will be made.

Present research at Mauna Loa centers about the IGY observational programs and on studies of the mountain climate and circulation, but additional work in several fields is planned.

Within its limitations of time, space, and personnel, the staff is prepared to offer housing and its other facilities to visiting scientists and to assist in the instrument-reading-and-servicing aspects of projects established there. Organizations and individuals desiring further information about the Observatory or the use of its facilities are invited to address their inquiries to the Director of Meteorological Research, U.S. Weather Bureau, Washington 25, D.C., or to the authors.

ACKNOWLEDGMENTS

The Mauna Loa Observatory owes its existence principally to Robert H. Simpson who, as Meteorologist-in-

Charge of the Weather Bureau's Pacific Supervisory Office, Honolulu, and afterwards, endeavored constantly to bring it into being; to his successors at Honolulu, Gordon D. Cartwright and Roy L. Fox, who dedicated much time and effort to the same end; to Ralph Stair of the National Bureau of Standards for his and his agency's cooperation in the construction of the present buildings; to Dr. Harry Wexler, Director of the Office of Meteorological Research of the Weather Bureau for his unstinting support and encouragement; and to the devoted work of the staffs of the Weather Bureau Airport Station, Hilo, and the Pacific Supervisory Office, Honolulu.

The thanks of the authors go also to Clifford M. Kutaka and to Raymond Sewake for their aid in compiling portions of the climatic data.

REFERENCES

1. Applied Physics Corporation, "Model 70 Infrared Analyzer," Pasadena, Calif., March 23, 1951.
2. Roy L. Fox, "The Mauna Loa Observatory," *Weatherwise*, vol. 9, No. 7, Oct. 1956, pp. 147–150.
3. Roy L. Fox, "New Mauna Loa Observatory Unit," *Nature*, vol. 178, No. 4545, Dec. 8, 1956, p. 1272.
4. S. Fritz, "The U. S. Special Meteorological Studies for the IGY," *Geophysical Monograph* No. 2, American Geophysical Union, 1958, pp. 161–168.
5. David S. Johnson, Progress Report on Radiometer Tests, U.S. Weather Bureau, Washington, D.C. (unpublished).
6. C. C. Kiess, C. H. Corliss, Harriet K. Kiess, and Edith L. R. Corliss, "High Dispersion Spectra of Mars," *Astrophysical Journal*, vol. 126, No. 3, Nov. 1957, pp. 579–584.
7. Dwight B. Kline and Glenn W. Brier, "A Note on Freezing Nuclei Anomalies," *Monthly Weather Review*, vol. 86, No. 9, Sept. 1958, pp. 329–332.
8. Lester Machta, "The Use of Radioactive Tracers in Meteorology," *Annals of the International Geophysical Year 1957/1958*, vol. V, Part V, Pergamon Press, 1958, pp. 309–312.
9. Ukichiro Nakaya, Juji Sugaya, and Mikio Shoda, "Report of the Mauna Loa Expedition in the Winter of 1956–1957," *Journal of the Faculty of Science*, Hokkaido University, Japan, Series II, vol. V, No. 1, March 1957, pp. 1–36.
10. E. J. Öpik, "Cosmic Sources of Deep-Sea Deposits," *Nature*, vol. 176, No. 4489, Nov. 12, 1955, p. 926.
11. Hans Pettersson, "Rate of Accretion of Cosmic Dust on the Earth," *Nature*, vol. 181, No. 4601, Feb. 1, 1958, p. 330.
12. Saul Price, "Notes on the Climate of Mauna Loa," *Proceedings*, Ninth Pacific Science Congress, Bangkok, November 1957 (in press).
13. K. R. Ramanathan, "Atmospheric Ozone and the General Circulation of the Atmosphere," *Scientific Proceedings*, UGGI, International Association of Meteorology, Rome, 1954, pp. 3–24.
14. Victor H. Regener, "Automatic Ozone Recorder," *Technical Manual*, Department of Physics, University of New Mexico, Oct. 30, 1956, pp. 1–29.
15. Special Committee for the International Geophysical Year, *Annals of the International Geophysical Year 1957/1958*, vol. V, Parts I, V, and VI, Pergamon Press, 1958.
16. Ralph Stair and Russell G. Johnston, "Some Studies of Atmospheric Transmittance on Mauna Loa," *Journal of Research of the National Bureau of Standards*, vol. 61, No. 5, Nov. 1958, pp. 419–426.
17. H. T. Stearns, "Geology of the Hawaiian Islands," *Bulletin 8*, Hawaii Division of Hydrography, 1946, pp. 1–106.
18. J. Warner, "An Instrument for the Measurement of Freezing Nucleus Concentration," *Bulletin de l'Observatoire du Puy de Dome*, No. 2, April/June 1957, pp. 33–46.
19. Harold W. Yates, "Recent Atmospheric Transmission Studies," paper presented at the 42d Annual Meeting, Optical Society of America, Cleveland, Ohio, Oct. 17–19, 1957. (Abstract in *Journal of the Optical Society of America*, vol. 47, No. 11, Nov. 1957, p. 1054.)

A NOMOGRAM FOR THE DETERMINATION OF SOLAR ALTITUDE AND AZIMUTH[1]

C. L. MATEER AND W. L. GODSON

Meteorological Service of Canada, Toronto, Canada

[Manuscript received August 22, 1958; revised December 3, 1958]

ABSTRACT

A combination nomogram is presented for the calculation of solar altitude and azimuth for any latitude, solar declination, and time of day.

1. INTRODUCTION

Meteorologists, and other scientists or engineers working in allied fields, frequently wish to determine the solar altitude and/or azimuth for various purposes. The present paper describes the construction of a combination nomogram for the calculation of both these quantities for any latitude, solar declination, and time of day.

2. DERIVATION AND CONSTRUCTION OF THE SOLAR ALTITUDE NOMOGRAM

The altitude of the sun is given by

$$\sin \alpha = \sin \phi \sin \delta + \cos \phi \cos \delta \cos h \tag{1}$$

where:

α = solar altitude (angular elevation above the horizon)
ϕ = geographic latitude of the observer
δ = declination of the sun
h = hour angle of the sun

Equation (1) may be compared with the relationship among the coordinates of three points $P_1(X_1, Y_1)$, $P_3(X_3, Y_3)$ and $P_5(0, Y_5)$, lying in a straight line, as illustrated in figure 1.

$$Y_5\left\{\frac{X_1}{X_3}-1\right\}-Y_3\frac{X_1}{X_3}+Y_1=0. \tag{2}$$

If we set

$$Y_1=K_1 \sin \alpha+C_1, \tag{3}$$

$$Y_5=K_5 \cos h+C_5, \tag{4}$$

and substitute these in (1) for $\sin \alpha$ and $\cos h$, we get

$$Y_5\left\{-\frac{K_1}{K_5}\cos \phi \cos \delta\right\}-\left\{C_1+K_1 \sin \phi \sin \delta - C_5\frac{K_1}{K_5}\cos \phi \cos \delta\right\}+Y_1=0. \tag{5}$$

If we now postulate that the left hand sides of (2) and (5) are to be identical, then

$$\frac{X_1}{X_3}-1=-\frac{K_1}{K_5}\cos \phi \cos \delta \tag{6}$$

$$Y_3\frac{X_1}{X_3}=C_1+K_1 \sin \phi \sin \delta-\frac{C_5K_1}{K_5}\cos \phi \cos \delta. \tag{7}$$

In summary, the following equations define the nomogram

$$Y_1=K_1 \sin \alpha+C_1$$

$$Y_5=K_5 \cos h+C_5$$

$$\frac{X_1}{X_3}=1-\frac{K_1}{K_5}\cos \phi \cos \delta \tag{8}$$

$$Y_3=C_5+\frac{X_3}{X_1}(C_1-C_5+K_1 \sin \phi \sin \delta).$$

K_1, C_1, K_5, C_5, X_1 are arbitrary factors, each having the dimension of length, which determine the size of the nomogram and the relative positions of the various scales.

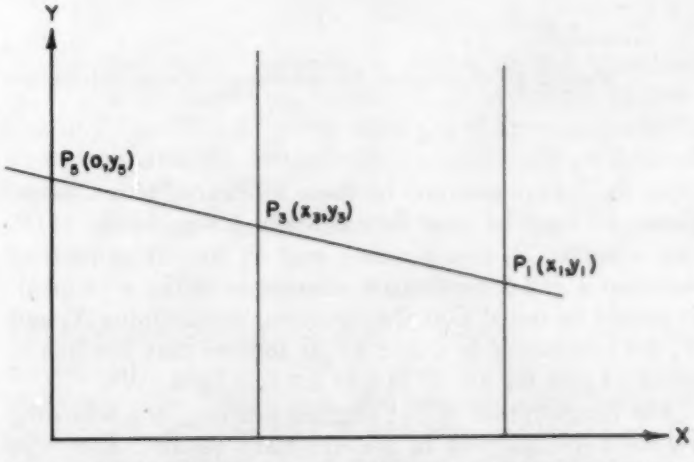

FIGURE 1.—Relationship among coordinates of three points lying in a straight line, similar to equation (2).

[1] Published by permission of the Director, Meteorological Branch, Department of Transport, Canada.

498746—59——3

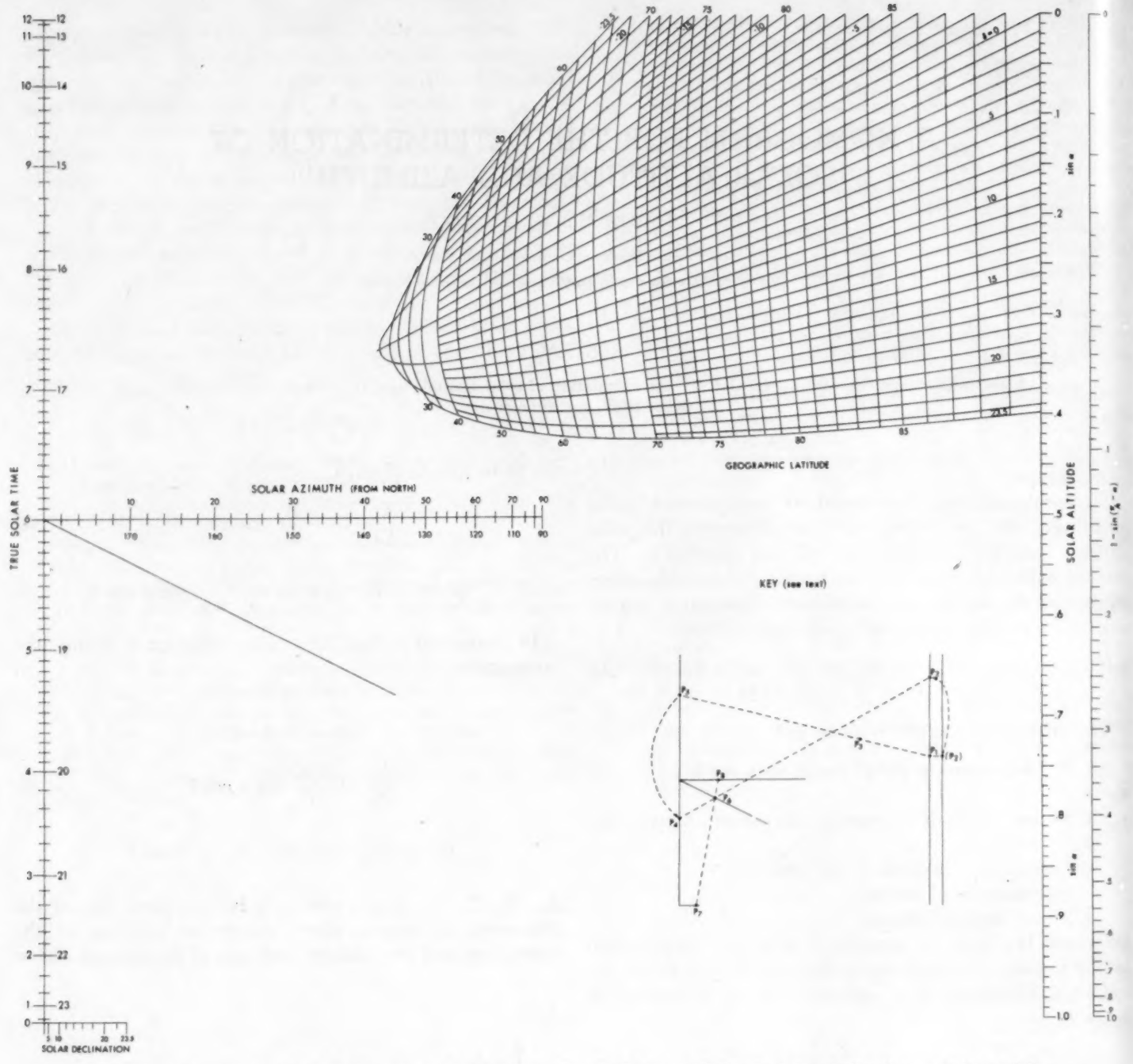

FIGURE 2.—Nomogram for calculation of solar altitude and azimuth for any latitude, solar declination, and time of day.

Once values are assigned to these arbitrary factors, equations (8) may be used to calculate the positions of P_1 (sin α scale), P_5 (cos h scale), and P_3 (family of lines of constant ϕ and δ, hereinafter referred to as the $\phi-\delta$ grid). It should be noted that the equations determining X_3 and Y_3 are symmetric in ϕ and δ. It follows that the line in the $\phi-\delta$ grid for $\phi=N°$ is also the line for $\delta=N°$.

For the purposes of the original drafting, the following values were assigned to the arbitrary factors: $K_1=-20$ inches, $C_1=10$ inches, $K_5=10$ inches, $C_5=0$, $X_1=20$ inches. The resulting nomogram is shown in Figure 2.[2]

3. USE OF THE SOLAR ALTITUDE NOMOGRAM

The True Solar Time (also referred to as Local Apparent Time or Sun-Dial Time) determines a point P_5 on the cos h scale, which is graduated directly in terms of time. The solar declination and geographic latitude determine a point P_3 on the $\phi-\delta$ grid. If P_3 and P_5 are joined by a straight line, which is extended to intersect the sin α scale

[2] A working size of the nomogram, about 9 in. x 9 in., will be made available in small quantities at no charge to interested readers. Address inquiries to Meteorological Service of Canada, 315 Bloor St. West, Toronto 5, Ontario.

at P_1, the solar altitude (actually sin α) may be read off directly at P_1.

For use at a single station, a nomogram may be constructed with only the latitude line for that station, calibrated re solar declination or directly re time of year. However, for single station work, the graph described by Schutte [2] is easier to construct and more convenient to use.

The solar altitude (sin α) scale may, of course, be labelled directly in terms of any quantity which is a single-valued function of solar altitude; e.g., optical air mass (average refraction assumed), CSCα at 22 km. (for ozone calculations), etc.

4. DISCUSSION OF ERRORS IN THE SOLAR ALTITUDE NOMOGRAM

The errors involved in the use of nomograms may be classified as follows:

(a) Errors in construction (drafting, printing, warping of paper).
(b) Errors in alignment (P_3, P_5).
(c) Errors in reading the answer (P_1).
(d) Curvature of straight-edge used.

The fourth type of error may be reduced by performing the calculation a second time, reversing the straight-edge end for end in doing so, and averaging the two answers.

The errors of types (b) and (c) result from the difficulty in precisely positioning the straight-edge directly over the points P_3 and P_5 and in reading the position of point P_1. In general these errors will depend on the angle at which the straight line P_5P_3 crosses the various scales. If we designate the standard error of positioning the straight line as Δ units of length, perpendicular to the line itself, at P_5 and P_3 and if β is the angle which P_5P_3 makes with the X-axis, then it may be shown that the standard error of P_1 due to alignment error is, in units of sin α,

$$\frac{\Delta \sec \beta}{K_1}\left(1-2\frac{K_1}{K_5}\cos\phi\cos\delta\right). \tag{9}$$

If we consider a further error in the final answer, due to the difficulty of reading off the position of P_1, equal to $\frac{\Delta \sec \beta}{K_1}$, then the final error is

$$\frac{\Delta \sec \beta}{K_1}\sqrt{1+\left(1-2\frac{K_1}{K_5}\cos\phi\cos\delta\right)^2}. \tag{10}$$

For the solar altitude nomogram in a convenient working size (about 10 in. x 10 in.), the maximum error occurs when $\phi=\delta=h=0$ and is 0.72Δ. The smallest error occurs when $\phi=90°$, $\beta=0$ and is 0.14Δ.

To provide a practical test of the accuracy obtained in using the nomogram, a set of 25 test computations was designed to sample all areas of the $\phi-\delta$ grid and the time and sin α axes. These were arranged in random order and given to four persons unfamiliar with the nomogram. After a few minutes instruction, each person was asked to go through all computations once, then to repeat the entire set with the straight-edge reversed. The two sets of answers were then compared and any deviations exceeding .007 were reconciled by repeat computations. Finally, the reconciled answers were averaged. The standard error σ, of the individual answer was as follows:

Observer A	(university graduate)	$\sigma=0.013$ (sin α units)
B	(" ")	0.010
C	(high school graduate)	0.013
D	(" " ")	0.012

If the errors in the determinations are classified according to geographic latitude, the following pattern of standard error emerges

$0 \leqq \phi < 20°$	$\sigma=0.027$ (cf. 0.72 Δ)
$20 \leqq \phi < 40$	$\sigma=0.012$
$40 \leqq \phi$	$\sigma=0.005$ (cf. 0.14 Δ)

Thus, neglecting errors in construction, one might infer a value of $\Delta=0.04$ in.

To give some idea of the accuracy obtainable by an experienced observer, one of the authors performed the same set of test computations. The standard error of these computations was 0.003 and a separation of errors according to latitude suggested a value of $\Delta=0.01$ in. Errors of this magnitude are quite acceptable for many meteorological and engineering uses.

5. SOLAR AZIMUTH NOMOGRAM

The solar azimuth angle, a (measured from north), is given by

$$\sin a=\sin h\frac{\cos\delta}{\cos\alpha} \tag{11}$$

For solution of this equation, it is convenient to use a proportional chart of the type described by Levens [1]. Such a chart is illustrated in skeleton form in figure 3. From pairs of similar triangles (AP_6P_2 and BP_6P_4, AP_6P_7 and BP_6P_8), it is readily seen that

$$\frac{BP_8}{AP_7}=\frac{BP_4}{AP_2}. \tag{12}$$

Interpreting these distances in terms of the variables (a, h, δ, α) as illustrated, equation (12) is directly equivalent to (11). The proportional chart of figure 3 has been incorporated in the solar altitude nomogram as described below.

The existing solar altitude scale may be used for cos α, noting that

$$1-\cos\alpha=1-\sin(\pi/2-\alpha). \tag{13}$$

An auxiliary scale, calibrated in $1-\sin(\pi/2-\alpha)$ is located immediately adjacent and parallel to the sin α scale. Once sin α is determined, the corresponding value of $1-\sin(\pi/2-\alpha)$ is read off on the adjacent scale and the sin α scale re-entered at this value. Let this point be P_2.

The existing time scale may also be used, since

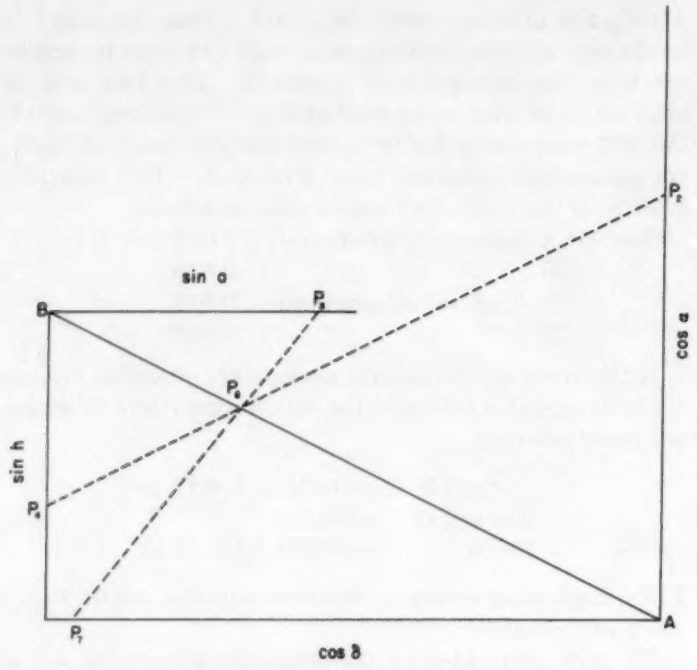

FIGURE 3.—Proportional chart for solution of equation (11).

$$\sin h = \cos(\pi/2 - h) = -\cos(3\pi/2 - h). \qquad (14)$$

Only the lower half of the cos h scale is used for the azimuth calculation. To determine the point P_4 at which one enters this scale, one must use either $\pm(h-6$ hr.) or $\pm(h-18$ hr.), whichever will give a point on the lower half of the time scale.

Points P_2 and P_4 are joined by a straight line which intersects the uncalibrated diagonal at P_6. Then P_6 is joined with P_7 on the solar declination scale at the bottom of the nomogram and the azimuth read off at P_8 on the azimuth scale.

In the Northern Hemisphere, the solar azimuth is measured from north and, during the time of year when $\delta > 0$, confusion may exist as to whether, for example, 70° or 110° should be read off the azimuth scale. When such confusion exists, the azimuth should be determined for a time a little closer to noon. If the new azimuth is closer to the 90° point, then the correct azimuth was 70°. If the new azimuth is slightly farther from the 90° point, then 110° is the correct azimuth.

ACKNOWLEDGMENT

The authors wish to acknowledge the assistance of Mr. Edward J. Truhlar with the calculations.

REFERENCES

1. A. S. Levens, *Nomography*, John Wiley and Sons, Inc., New York, 1948, p. 76.
2. K. Schutte, "Ein Einfaches Graphisches Verfahren zur Bestimmung von Hohe und Azimut der Sonne," *Meteorologisches Zeitschrift*, vol. 48, 1931, pp. 314–319.

FORECASTING MINIMUM TEMPERATURES ON CLEAR WINTER NIGHTS IN AN ARID REGION

A Comparison of Several Climatological Aids

PAUL C. KANGIESER

U. S. Weather Bureau Airport Station, Phoenix, Ariz.

[Manuscript received October 7, 1957; revised July 16, 1958]

ABSTRACT

Minimum temperature formulas for clear nights in December, January, and February are developed by the Young method and tested on both original and test data. The results of these tests lead to a discussion of some weaknesses of the "method of arbitrary corrections." Jacobs' graphical adaptation of Brunt's equation is tested (a) using experimentally determined values for the local soil constants to compute the "effective" soil factor, and (b) using a soil factor determined empirically for local meteorological data. With Brunt's equation as a model, the physical justification for Young's method is discussed, and a more direct approach suggested using the evening dry bulb and wet bulb temperatures and a modern method of data analysis. There is further discussion of some implicit assumptions in the Young method of analysis and an attempt is made to see if these assumptions are satisfied by the analysis performed in combining the evening dry bulb and wet bulb temperatures and the expected morning minimum using modern methods. In the Appendix, the application of the latter method is extended to cloudy nights and performance comparisons with official forecasts are made and discussed.

1. INTRODUCTION

Meteorologists in many parts of the world have concerned themselves during the past half century with the problem of forecasting the minimum temperature using hygrometric data [13]. Most of the methods apply best on clear nights, and attempt to provide the forecaster with an estimate of the fall of temperature to be expected during the night (under average radiation conditions), using surface temperature and hygrometric readings near the time of sunset. Most of the methods do not provide a completely objective forecast, but encourage the forecaster to modify the formula value subjectively on the basis of expected wind and sky conditions during the night; hence, they may be called "climatological aids" to forecasting.

In the Salt River Valley of Arizona, minimum temperatures are of major concern to citrus growers during the winter season. Many of the conditions required for the successful functioning of most of the formulas are satisfied locally on the majority of winter nights because (1) the skies are usually clear, (2) surface winds are light, and (3) the air is relatively free from pollutants. Hence, this should be a good place to compare the performance of hygrometric relationships.

Many minimum temperature studies in the past have been concerned only with temperatures in the lower ranges, since those are the cases of primary interest in frost forecasting. The present study is made with the forecasting program of a First Order Weather Bureau Station in mind, and purposely includes temperatures in all ranges. Daily forecasts for such a station are given press, radio, and television distribution, so that minimum temperature forecasts in higher ranges, too, are of considerable operational importance.

TABLE 1.—*Data periods used in the study.*

Original Data			Test Data		
Month	Years included	No. cases	Month	Years included	No. cases
Dec.	1948, '50, '52, '54, '56	98	Dec.	1949, '51, '53, '55	88
Jan.	1949, '51, '53, '55, '57	85	Jan.	1950, '52, '54, '56	72
Feb.	1949, '51, '53, '55, '57	88	Feb.	1950, '52, '54, '56	71

2. DATA USED FOR THE STUDY

Observations made at the Weather Bureau Airport Station in Phoenix during December, January, and February over a 9-year period, were used in making the comparisons. These data were divided into two groups as indicated in table 1.

Alternate years were used in each group to reduce the effects of any year-to-year persistence that might be present in the data. Only data for clear nights were used: a night was called "clear" if the mean sky coverage for the nine hourly observations (0030–0830 MST) was in the range 0–3/10. Hence, if any of the derived relationships are applied to operational forecasting, the forecaster is left to make the decision of whether or not the night will be clear.

498746—59——4

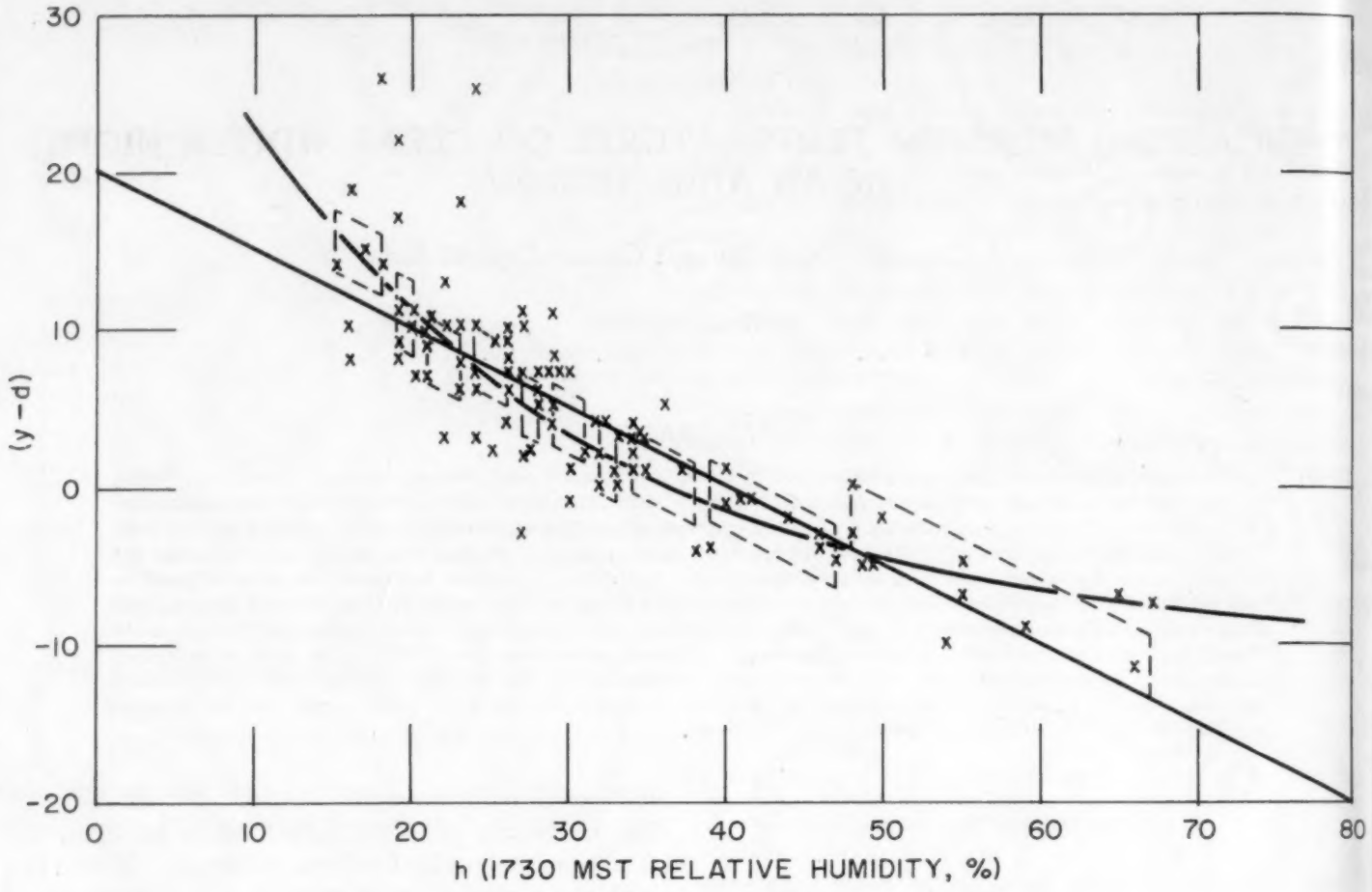

FIGURE 1.—Graph of $(y-d)$ against h for the December original data.

3. COMPARISON OF THE METHODS

YOUNG'S METHOD

Some years ago, Ellison [3] made a rather extensive comparison of a number of hygrometric formulas by applying them to the same set of data. On the basis of that study, he concluded that the Young formula gave the best results, especially if modified by the "method of arbitrary corrections." Therefore, the first method tested in the present study was Young's formula based on local data.

Individual Young formulas for clear nights were constructed using the original data for December, January, and February, respectively. Complete instructions for the development of the relationship are given in [3]; however, a brief description of the procedure used will be given here. First a graph was plotted using $(y-d)$ as the ordinate and h as the abscissa, where h is the 1730 MST relative humidity percent, d is the 1730 MST dew point (°F.), and y is the observed minimum temperature (°F.) the following morning. A straight line of best fit (minimizing the absolute error) was then fitted by inspection. Figure 1 shows the graph for the December original data. Similar graphs prepared for January and February are not reproduced here.

Next the equation of the straight line was written in the form recommended in [3], known as the "Donnel formula,"

$$y=d-\frac{h-n_1}{n_2} \tag{1}$$

where n_1 is the h-intercept and n_2 is the *negative* of the reciprocal of the slope of the line.

The final form recommended [3] for the equation is

$$y=d-\frac{h-n_1}{n_2}+V_d+V_h \tag{1A}$$

where V_d and V_h are correction factors derived from the original dew point and relative humidity data, respectively, as follows:

1. Values of d and h for each day were written on cards, along with the date.

2. Using the straight line formula (1), the formula minimum temperature was calculated, and the departure between this and the observed minimum temperature was written on each card.

3. The cards were then arranged in the order of increasing relative humidity. At intervals of approximately 10 cards, the average departure of the formula minimum

TABLE 2.—*Formula for the minimum temperature, y, for December, and set of arbitrary corrections*

$$y=d-\frac{h-40}{2}+V_d+V_h$$

h	V_h	d	V_d
15–18	+3.5	13–19	+1.5
19–20	+1.5	20–24	−0.5
21–23	−0.5	25–28	+0.5
24–26	+0.5	29–30	−0.5
27–28	−1.0	31	+1.5
29–31	−0.5	32–33	−0.5
32–33	−2.0	34	0
34–38	−1.0	35–36	+0.5
39–47	−0.5	37–38	−2.5
48–67+	+2.5	39–46+	−0.5

temperature estimate from the observed minimum temperature was calculated. This was then used as the arbitrary correction to be applied to the formula over the range of relative humidity indicated by the group of cards. This correction was applied to the original formula estimate and a new departure was calculated.

4. After the relative humidity corrections were determined and applied, the cards were arranged in the order of increasing dew point. The process just outlined was repeated, and the arbitrary correction to be applied to the formula over a given range of dew point was computed.

The formula for December and the set of arbitrary corrections are given in table 2. Similar formulas were derived for January and February. In applying the formulas to the data it is not necessary to solve the equations each time, as it is simpler to prepare a table of values of $(y-d)$ against h from the straight line, then add the corrective factors algebraically to the tabular value. This procedure is especially helpful if a curvilinear relationship is drawn to the data as on figure 1.

From these relationships, the minimum temperature was calculated on clear nights, using the original data and the independent data. The average absolute forecast error for each group is shown in table 4. One set of values was computed using the straight line formulas alone (without the correction factors V_d and V_h) and another set was computed using the complete relationship. The former are labeled "uncorrected" and the latter "corrected." Notice that the application of the method of arbitrary corrections to the original data produced a marked increase in skill but that no increase resulted when the method was applied to test data.

Next a curved line was fitted by inspection to the same data for each month (the line for the December data is shown in figure 1). The results obtained by testing each of these lines on both original and test data are given in table 4 under the heading, "Young's method, curved lines, corrected." Again, the method of arbitrary corrections was applied to forecasts made from these lines, but this time the corrections were rounded off to the nearest whole degree. The correction values for the December data only are shown in table 3. Again no significant increase

TABLE 3.—*Correction values for Young's method, curved lines, December data*

h	V_h	d	V_d
15–19	0	13–19	+1
20–22	−2	20–24	0
23–24	+1	25–28	0
25–26	+1	29–30	0
27–28	+1	31	+1
29–31	+1	32–33	0
32–33	0	34	0
34–38	+1	35–36	+1
39–47	0	37–38	−2
48–67+	0	39–46	−1

occurred when the corrections were applied to test data (see table 4 under heading, "Young's method, curved lines, corrected").

To understand this lack of improvement from the use of the method of arbitrary corrections, one must understand what the method does. As pointed out in [8], application of the method to all possible combinations of values of d and h, using finite intervals of these, yields a series of straight lines that are always parallel to the original straight line. In [8] adjacent end-points of the intervals were connected with straight lines, thereby giving a continuous, irregular line. Such a procedure has no meaning, however, because there is no way equation (1A) can generate solutions for line segments with slopes different from that of the straight line given by the part of the formula without the correction factors. Thus a series of disconnected straight lines should be drawn.

Instead of lines for all possible combinations of V_d and V_h, only the top and bottom of the series of lines were entered in figure 1, so that the areas within the rectangles contain all solutions possible with the December formula and tabulated corrections. The top of the farthest rectangle to the left (corresponding to $15 \geq h \geq 18$) is obtained from the December formula using $V_h=3.5$, $V_d=1.5$; while the bottom is obtained using the lowest tabulated value for V_d (-2.5). The rectangles for the other intervals of h and d used in the table were drawn on figure 1 in the same fashion.

Notice that the general pattern of the rectangular areas indicates a curvilinear relationship that follows somewhat the curved line fitted by inspection, but there is considerable up and down fluctuation which follows rather faithfully the sampling variation in the original data. This same sampling variation is then imposed on the test sample, which may explain the fact that no increase in skill was obtained over the linear relationship; applying this original sampling variation to the test sample nearly counterbalances the increase in skill contributed by the general curvilinear pattern followed by the areas. Obviously, correction for the sampling variation can cause a significant increase in skill only if the method is tested on the original data alone as was done in [3].

Smith [10] suggested that a curve of the second degree, drawn on the graph of $(y-d)$ against h, will probably yield better results, in the long run, than the Young formula. This seems borne out by the verification scores

TABLE 4.—*Comparison of average absolute error (° F.) obtained on samples of original and test data using the various methods*

	Young's method (straight lines)				Young's method (curved lines)				Jacob's method		Wet bulb vs. dry bulb method	
	Uncorrected		Corrected		Uncorrected		Corrected					
	Original data	Test data	Original data	Test data	Original data	Test data	Original data	Test data	Original data	Test data	Original data	Test data
December	2.7	3.3	2.4	3.2	2.7	2.9	2.5	2.8	3.2	3.7	2.3	2.7
January	3.6	3.5	2.7	4.0	3.1	2.9	2.5	3.0	4.4	3.0	2.2	2.7
February	3.3	3.5	2.5	3.0	2.5	2.8	2.1	2.7	3.8	3.9	2.3	2.1
Average	3.2	3.4	2.5	3.4	2.8	2.8	2.3	2.8	3.8	3.6	2.3	2.5

in table 1, because the curved line *without* correction factors gives a higher score on test data than the linear relationship *with* the correction factors. Note also that there is little difference between the scores on original and test data for the curved line, and on the test data for the curve with correction factors applied; however, the correction factors applied to the original data improved the skill considerably. This indicates that the correction factors are primarily correcting for the sampling variation in the original data, and that the curve is doing as good a job by itself of estimating the relationship as the curve with the factors applied.

JACOBS' METHOD

Another aid to forecasting the minimum temperature, used with some success in the past, is Jacob's [6] diagram, which is based on a formula for the temperature change at a key station in El Centro, Calif.:

$$\Delta t_1 = 12.32(0.56 - 0.08\sqrt{e})\sqrt{t} \tag{2}$$

where e is the vapor pressure (mb.), Δt_1 is the temperature drop (° C.), and t is the time (hours) after sunset (or length of night). This formula was derived, in turn, from a formula by Brunt [1]

$$y = T_o - \frac{2\sigma T^4}{\sqrt{\pi}}\left(\frac{1-a-b\sqrt{e}}{\rho_1 c_1\sqrt{k_1}}\right)\sqrt{t}. \tag{3}$$

In (3), ρ_1 is the soil density, c_1 is the specific heat of the soil, and k_1 is the thermal conductivity of the soil, σ is Stefan's constant, T is the radiative temperature (mean temperature during the night, for practical purposes), T_o is the temperature at sunset, and y is the forecast minimum temperature.[1] Jacobs [6] constructed a set of graphs based on formula (2) and provided factors to correct for variations in T and for different values of the "effective" soil factor (s), where $s=\sqrt{\pi}\rho_1 c_1\sqrt{k_1}$. a and b are constants in an empirical equation developed by Brunt [1] which expresses the relationship between the surface vapor pressure, the total long-wave radiation downward from the atmosphere, and the total black-body radiation at a given surface temperature on clear nights. The values of a and b used here are those used by Jacobs ($a = 0.44$, $b = 0.08$).

[1] Jacobs used T_1 for the minimum temperature, but y will be used here to be consistent with the notation used above.

Local average values of $\rho_1=2.70$ gm. cm.$^{-3}$ and $c_1=0.20$ cal. gm.$^{-1}$ °C.$^{-1}$ were obtained from the College of Agriculture at Arizona State University. The mean value of $k_1=4.7\times10^{-4}$ cal. sec.$^{-1}$ cm.$^{-1}$ °C.$^{-1}$ given by Jacobs [5] was used, along with a value of $t=14.0$ hr. The shelter temperature at 1730 MST was substituted for T_o and the vapor pressure at the same time was used for e.

In computing formula (2), Jacobs used a value of $T=280°$ AA. In the present study, a value of $T=283°$ AA was used since the mean nighttime temperature at Phoenix during the winter averages near 50° F. Actually, the numerical value of T used in developing the basic formula is arbitrary, since a correction is ultimately included for the observed (or forecast) mean temperature during the night; it becomes important only if the correction is not applied.

The values of the variables and constants given above, gave the following formula for Phoenix:

$$T_o - y = 16.1(0.56 - 0.08\sqrt{e})\sqrt{t}. \tag{4}$$

This equation expresses (T_o-y) in degrees Celsius. Curve A on figure 2 gives (T_o-y) in degrees Fahrenheit, using a constant value of $t=14.0$ hours. Figure 3 gives the value of the correction factor (f) by which the value of (T_o-y) from figure 2 must be multiplied to correct for the actual mean temperature during the night. In the verification, the observed value of $T=\frac{1}{2}(T_o+y)$ was used as the mean temperature during the night. Formula (4) was verified only on the December original data, since it became obvious during the verification that the formula was consistently forecasting minimum temperatures that were much too low. An average error of 11.5° F. was obtained.

Brunt [1] states that the chief difficulty in the way of using formula (3) for forecasting the night minimum temperature lies in the uncertainty of the value of the coefficient $\rho_1 c_1\sqrt{k_1}$, and that the addition of 20 percent of water to dry soil increases this factor five-fold. Jacobs [6] suggests that these factors can probably best be derived empirically, so equation (3) was written in the form

$$\frac{1}{\rho_1 c_1\sqrt{k_1}} = -\frac{\frac{\sqrt{\pi}}{2\sigma T^4\sqrt{t}}(y-T_o)}{(1-a)-b\sqrt{e}}. \tag{5}$$

From the values stated above of σ, T, t, a and b, and observed values of y, T_o, and e (1730 MST) for all clear nights

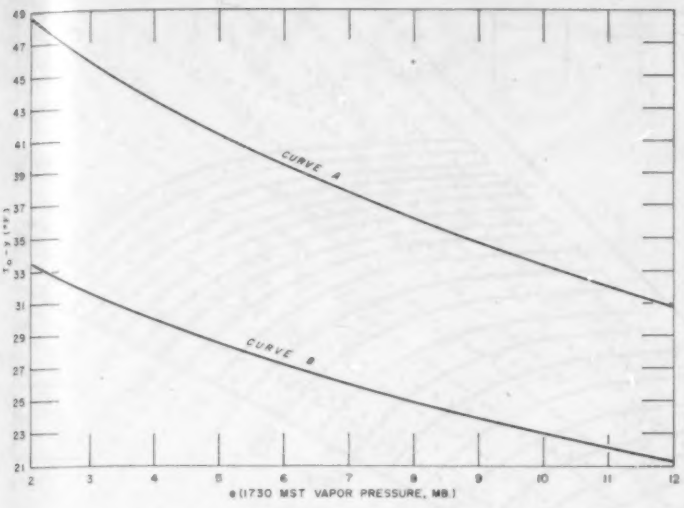

FIGURE 2.—(T_o-y) plotted against vapor pressure (e) at 1730 MST. Curve A=curve for equation (4). Curve B=curve for equation (6).

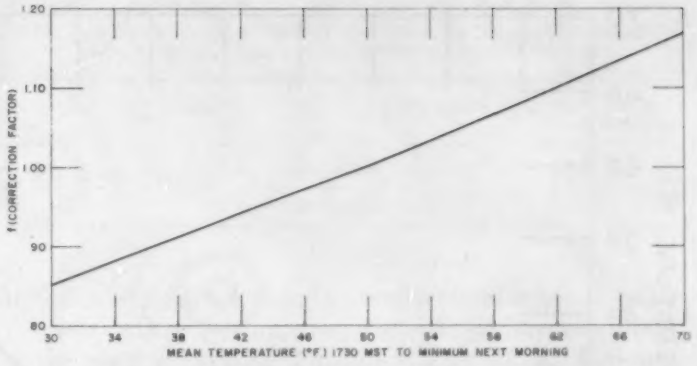

FIGURE 3.—Correction factor (f) by which (T_o-y) from equations (4) and (6) should be multiplied to correct for the mean temperature during the night.

in December, January, and February of the original data, a value of $1/\rho_1 c_1\sqrt{k_1}$ was computed for each of the 271 nights. A frequency polygon was constructed from these values and the median value computed. The distribution of values turned out to be very regular (little or no skewness) so that the mean and the median coincided at 33.5. From the frequency polygon, a percentile estimate of the standard deviation using 10 percentiles [2] gave a value of 7.5. This estimate (statistical efficiency 0.92) of the standard deviation is included only to give some idea of the spread of the data about the mean value.

The median value of $1/\rho_1 c_1\sqrt{k_1}$ was then substituted into equation (3) and by rearrangement a new equation similar to (4) was obtained:

$$T_o-y=11.1\ (0.56-0.08\sqrt{e})\ \sqrt{t}. \qquad (6)$$

Like equation (4), this equation gives (T_o-y) in degrees Celsius, assuming a mean temperature during the night of 283° AA. Curve B on figure 2 gives expected values of (T_o-y) in degrees Fahrenheit, using a constant value of t=14.0 hr. Figure 3 may be used in the same manner as with equation (4) to correct for the observed mean temperature during the night.

As in the case of equation (4), the verification of this equation was carried out using observed values of $T=\frac{1}{2}(T_o+y)$. As can be seen in table 4, the results are considerably improved over those of equation (4). The use of Jacobs' equation on an operational basis requires, in addition to a forecast of sky condition, an estimate of the mean temperature during the night; however, using the observed 1730 MST temperature and a rough estimate of the minimum temperature to compute $T=\frac{1}{2}(T_o+y)$ would probably have given results on the same data nearly comparable to those obtained here.

A MORE DIRECT APPROACH

A climatological aid for forecasting the minimum temperature should be a simple relationship based on evening data, which the forecaster can use for guidance in making his forecast. Most of the methods developed in past years have used evening temperature and moisture parameters to forecast the minimum temperature the following morning, and physical justification for this procedure can be found in Brunt's equation. In equation (3) all variables are assumed to be constants with the exception of y, T_o, T, t, and e. We have seen, however, that T may be closely approximated by $(y+T_o)/2$, and t may be taken as a constant (14.0 hr. was used above). Hence, the only variables left are y, T_o, and e. Young's method essentially substitutes two other functions of T_o and e; namely, h and d. Another possibility for a 3-variable combination that seems quite feasible, in terms of Brunt's equation, is y, T_o, and the wet bulb temperature T_w. Both T_o and T_w are measured directly in the instrument shelter and so are somewhat easier to use on an operational basis than d and h.

Given three variables, T_o, T_w, and y, between which a joint relationship is suspected, there are a number of ways to approximate this relationship [4], [7]. One of the most straightforward, however, is to plot T_o along one coordinate axis, T_w along the other, and the numerical value of y at the intersection point in the field of the graph corresponding to particular values of T_o, T_w. Isopleths of constant values of y may then be drawn by one of several methods [4], [7]. A diagram of this type is shown in figure 4, based on the 271 cases of original data for December, January, and February combined. The isopleths were drawn by the method of substratification and successive graphical approximation described in [4].

The advantage of this type of combination of variables is that no initial assumption is made about the form of the relationship, and the data are given freedom to indicate their relationship within the limitations of the sample size. This is in contrast to the Young formula, for example, which plots two variables along one axis as $(y-d)$, and thereby implicitly assumes that these two variables have equal weight in the relationship with h, and that the regression of y on d (or vice versa) is linear for constant h.

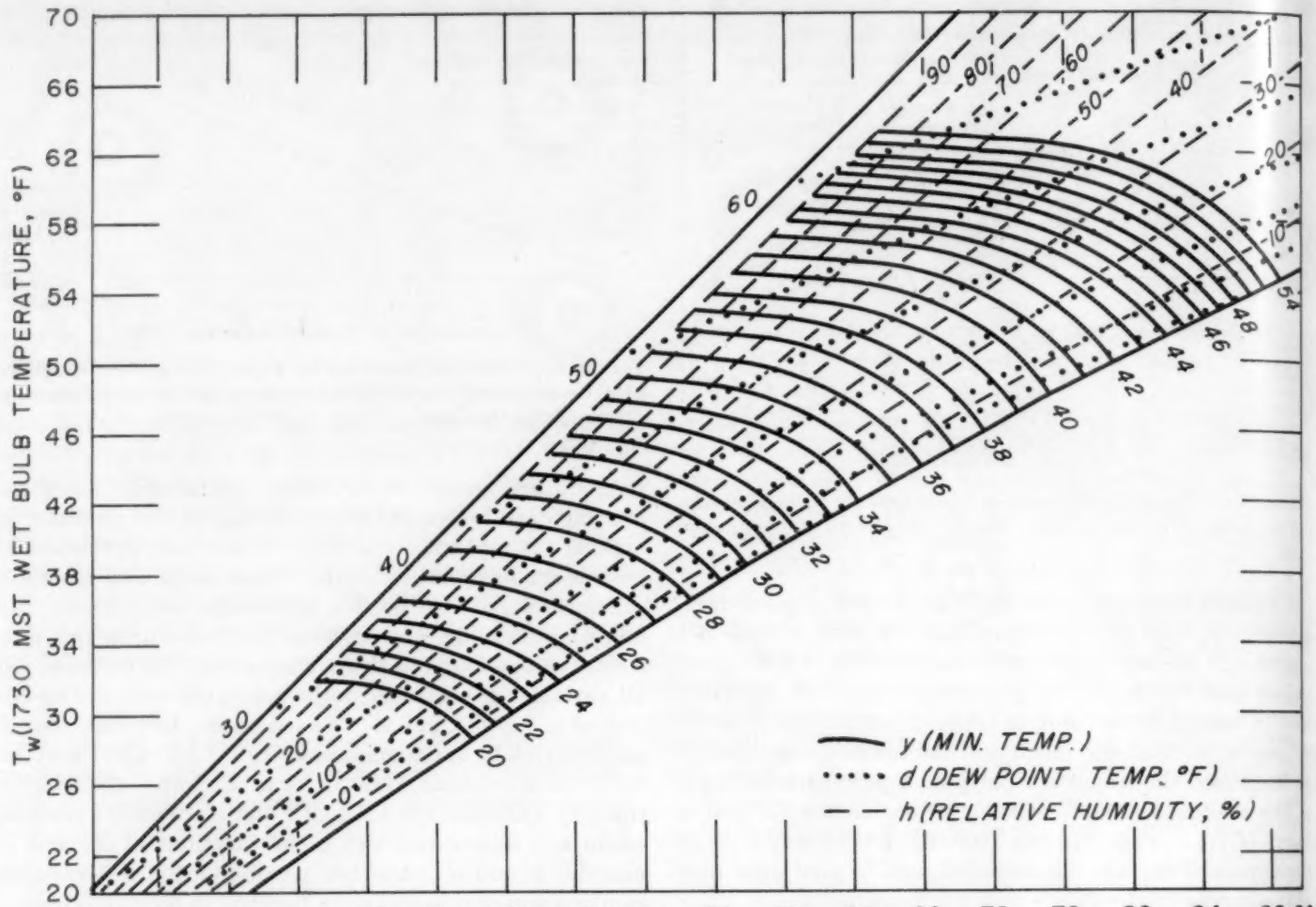

FIGURE 4.—Graph showing the estimated joint relationship between T_0, T_w, and y on clear nights. Lines of constant d and h were added using hygrometric table after analysis was performed.

These assumptions become readily apparent if the relationship between y, d, and h is examined on a graph using $(y-d)$ as the ordinate and h as the absicssa. Such a relationship can be expressed in the following general functional form,

$$y-d=f(h) \tag{7}$$

or,

$$y=f(h)+d \tag{8}$$

where $f(h)$ is assumed to be a continuous function for all values.

Now consider the effect of holding h constant,

$$y=\text{constant}+d. \tag{9}$$

The linearity between y and d for constant h and the assumption of equal weight of y and d with respect to h are shown by (9), and can be graphically illustrated on a diagram of the kind shown in figure 4, by using y as the ordinate, d as abscissa, and h in the field of the diagram. Such a diagram will always have the following set of characteristics no matter how complicated the curve drawn on figure 1 to indicate the relationship between y, d, and h, lines of constant h will always be straight lines, and the slope of these lines will always be 1. As an example, the relationship between y, d, and h shown by the curved line in figure 1, is converted into this kind of diagram in figure 5 (solid lines).

Since the Young method has the implicit assumptions mentioned above, it might be of interest to see how well these assumptions are satisfied by the analysis in figure 4, since that analysis was carried out unencumbered by those assumptions. To do this, however, we must convert the relationship shown in figure 4 into one between y, d, and h. This can be done simply by drawing lines of constant d and h in figure 4 using a hygrometric table. These lines can then be used to graph the relationship between y, d, and h in figure 5 (dashed lines), for a comparison with the lines (solid) drawn using the curvilinear relationship in figure 1. Obviously, such a comparison can be used only to indicate differences between the results of the two methods on this sample of data, since neither one is known to be "correct." The dashed lines, which were free to assume

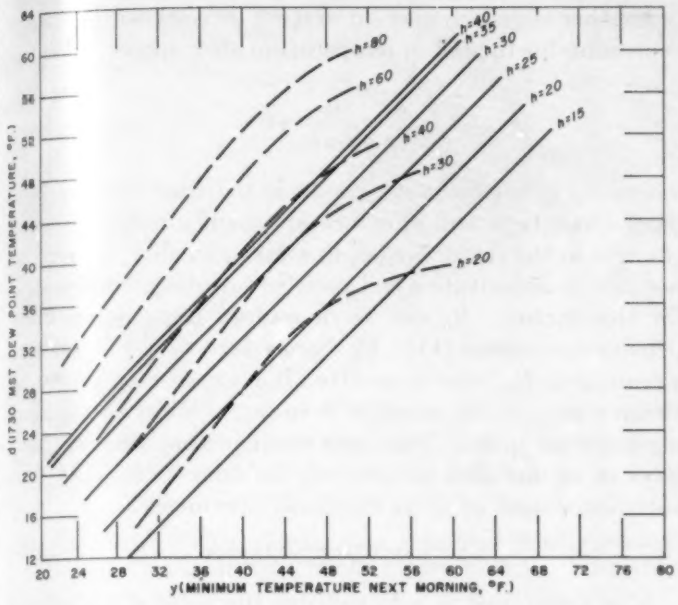

FIGURE 5.—Graph showing relationship between d, y, and h for clear cases. Solid lines show the relationship represented by the curve in figure 1. Dashed lines show the relationship from the analysis on figure 4.

any configuration in figure 5, seem quite straight for values of y less than about 40°. Thus the assumption of linearity of the regression of y on d for constant h seems fulfilled by the figure 4 analysis for lower values of y, but seems to break down at higher values of y (and higher values of d and h).

Young [12] found that forecasts made from a straight line relationship on a graph like figure 1 were considerably in error at high values of d and h (and also for very low values) and developed the method of arbitrary corrections to correct for this. It should be emphasized here, however, that the statement above about the indicated lack of linearity in figure 5, should not be confused with Young's finding. The lack of linearity indicated in figure 5 is between the regression of y on d for constant h, and if real, cannot be corrected by any method as long as the basic graph is like that used in figure 1. Obviously, the method of arbitrary corrections also operates within the framework of the two assumptions described by equation (9).

For the dashed lines in figure 5, the slope is approximately 1.3 for values of y less than about 40. For higher values of y, the slope becomes variable.

Thus the assumptions implicit in the Young method are only approximately fulfilled by the original analysis in figure 4. Although we cannot draw definite conclusions from the comparison in figure 5, it is possible that some of the difference in skill on the test data between the analysis in figure 1 and that in figure 4 (see table 4) is due to a lack of conformity of the data to the assumptions made in figure 1.

To provide some standard of comparison for the performance of figure 4, temperature estimates made using 1730 MST data were compared with official forecasts made by the staff at WBAS Phoenix. The official forecasts of the minimum temperature the following morning are made on an operational basis at 1930 MST each evening. The average absolute error by seasons is shown in table 5 for all clear cases. The seasons used were from the test sample for figure 4 (1954 season=Dec. 1953, Jan. and Feb. 1954; 1956 season=Dec. 1955, Jan. and Feb. 1956; etc.). It should be pointed out in this comparison, that the climatological aid "knew" that the night would be clear, while the staff forecasters did not.

TABLE 5.—*Comparison of average absolute error for the climatological aid (T_o vs. T_w) and official forecasts for clear nights*

Season	No. cases	T_o vs. T_w	Official forecasts
1954	63	2.7	3.8
1956	57	2.2	3.2
1958	53	2.2	2.2

It is of interest to note that the climatological aid averaged approximately 1° F. better than the official forecasts in the first two seasons, but in the last season the skill was about the same for both. During the 1958 season the Meteorologist in Charge placed the climatological aid in the station forecast manual and the forecasters used it on a discretionary basis. There is no way of determining what part (if any) of the improvement in skill shown in the 1958 season was due to its use.

4. CONCLUSIONS

YOUNG'S METHOD

In this method a graphical combination of y, d, and h is performed, but the combination is done within the framework of the following assumptions: (1) the regression of y on d, for constant h, is linear, and (2) y and d have equal weight in the relationship with h. If these assumptions are not fulfilled by the "population," a loss in skill can be expected over that obtained by a method of analysis allowing greater degrees of freedom.

Another logical combination of variables, in terms of Brunt's equation, is T_o, T_w, and y. An advantage of this combination is that the independent variables (T_o and T_w) are measured directly in the instrument shelter. These variables were combined on a graph using T_w as ordinate and T_o as abscissa. If estimates of y are desired in terms of d and h, as in Young's method, it is only necessary to add lines of constant d and h to this diagram with a hygrometric table.

With Brunt's equation as a working physical model, Young's method which combines h, d, and y is seen to be essentially the same as the method employing T_o, T_w, and y. It is possible that the improvement in skill shown on test data by the latter method is largely due to the use of an improved method of data analysis. Whether or not this is true, we have seen that the Young method

of combining d, h, and y introduces assumptions for which no *a priori* physical reasons have been given. There seems little reason for imposing these assumptions today, when we have a number of good methods for estimating the joint relationship between several variables which do not require such arbitrary restrictions.

A relationship between y, d, and h was derived using a method of analysis that did not arbitrarily place these two restrictions on the data. The following conclusions were drawn for the particular analysis performed on this particular set of data: (1) assumption No. 1 was well satisfied for observed minima below about 40° F. but broke down at higher minima, and (2) assumption No. 2 was not quite as well satisfied, even at temperatures in the lower ranges.

If the Young method of combining y, d, and h is used, it is recommended that instead of preserving the original first-degree estimate of the plotted relationship between $(y-d)$ and h by applying the corrections in the form of formula (1A), a curvilinear relationship of the second degree be drawn. Forecasts made from this line will probably be subject to less loss in skill caused by imposing original-data sampling variation on future samples.

JACOBS' METHOD

This method does not seem to be more capable of universal application (application without determining local constants by data processing) than other methods. This may be due primarily to the difficulty of obtaining reliable estimates of the soil factors, which probably not only undergo considerable seasonal variation, but also may differ, on the average, between clear and cloudy nights.

A MORE DIRECT APPROACH

Inspection of Brunt's equation (3) provides a physical justification for using the evening dry bulb temperature (T_o) and the evening vapor pressure (e) to forecast the minimum temperature the next morning (y). Since dew point (d) and relative humidity (h) are functions of T_o and e, the combination of d, h, and y also seems logical, but it is recommended that a method of estimating the joint relationship between these variables be used that does not place unnecessary restrictions on the data.

5. SUGGESTIONS FOR FURTHER RESEARCH

This study has discussed methods which, in effect, use T_o and e to estimate y. Obviously, there are many other variables of great importance, but the introduction of these into the relationship was beyond the scope of this project. Some of these important additional variables are (1) wind, (2) turbulence, (3) advection, (4) soil moisture, (5) soil temperature, (6) air temperature aloft, and (7) moisture distribution aloft. One approach to future research in this field might be to incorporate these variables into the relationship, perhaps using the "residual method" [9], which has the advantage of showing whether an additional variable improves a forecast based on other variables.

Another approach may be to work directly with Brunt's expression for the fall in temperature after sunset, which is

$$\frac{2}{\sqrt{\pi}} \frac{R_N}{\rho_1 c_1 \sqrt{k_1}} \sqrt{t}$$

where R_N is net radiation, and t is the time after sunset. Since changes in soil moisture are mainly responsible for changes in the factor $\rho_1 c_1 \sqrt{k_1}$ in a given locality, it may be possible to substitute a soil moisture reading, empirically, for this factor. R_N can be measured using fairly inexpensive equipment [11]. One procedure would be to take a reading of R_N near or shortly after sunset and, following Brunt's suggestion, consider it to be constant throughout a given clear night. Forecasts made in this fashion would have to be modified subjectively for advection, wind, and turbulence, just as those discussed previously.

ACKNOWLEDGMENT

It is a pleasure to acknowledge the helpful discussions during this project with Mr. Louis R. Jurwitz, Meteorologist in Charge, Weather Bureau Airport Station, Phoenix and with members of his staff.

APPENDIX

EXTENSION OF THE METHOD IN FIGURE 4 TO CLOUDY NIGHTS

To extend the usefulness of the climatological aid, graphs similar to figure 4 were prepared for two other classes of nights, as follows:

Class 1. This class contains principally nights with high broken to overcast conditions and with no persistent ceiling below 10,000 feet. Criteria: on the morning following the evening on which the forecast was made, the observed mean sky coverage on the nine hourly observations 0030–0830 MST, inclusive, was in the range 4/10–10/10 *and* a ceiling of 10,000 feet or less was reported on no more than 4 of these observations.

Class 2. This class contains principally nights with broken to overcast skies and with a persistent ceiling below 10,000 feet. Criteria: on the morning following the evening on which the forecast was made, the observed mean sky coverage on the nine hourly observations 0030–0830 MST, inclusive, was in the range 4/10–10/10 *and* a ceiling of 10,000 feet or less was reported on 5 or more of these observations.

It will be noted that on figure 4 the minimum temperature lines are not extended into the region of the graph above a relative humidity of 90 percent. Extension of the lines into that region would have little meaning because a relative humidity that high in the early evening usually leads to ground fog by morning, automatically placing the case in the "cloudy, class 2" category. For this same reason there were practically no observed cases in this region of the diagram for the "cloudy, class 1" category, (fig. A–1) so the minimum temperature lines above a relative humidity of 90 percent were omitted on this diagram also.

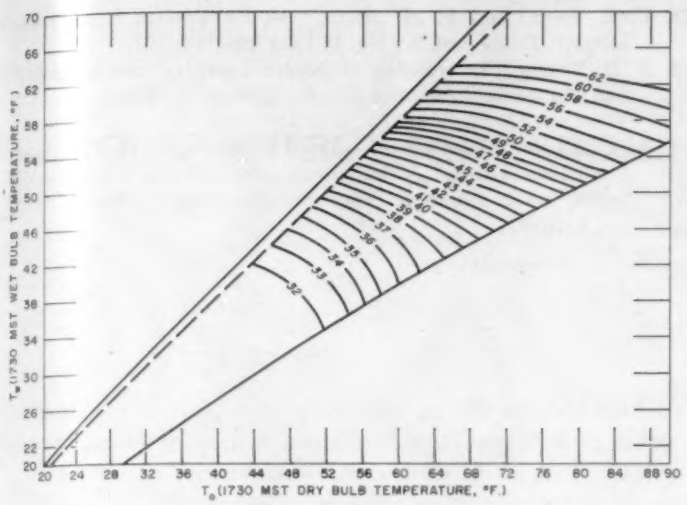

FIGURE A–1.—Graph showing the estimated joint relationship between T_o, T_w, and y on cloudy nights (class 1). Lines of constant y (estimated) are drawn in the field of the diagram.

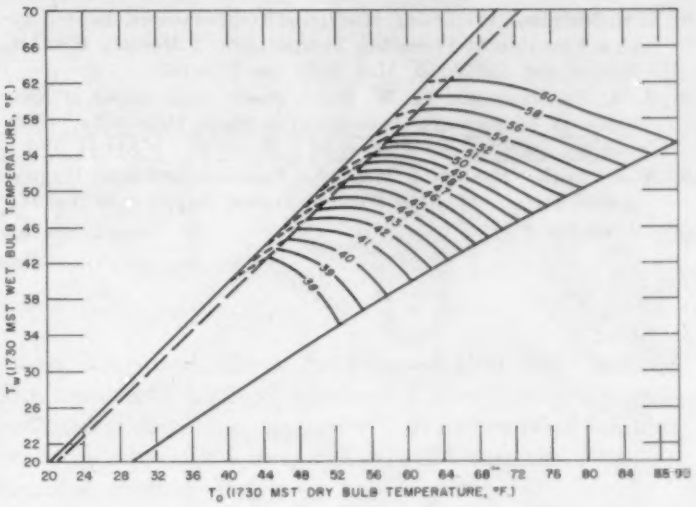

FIGURE A–2.—Graph showing estimated joint relationship between T_o, T_w, and y for cloudy nights (class 2). Lines of constant y (estimated) are drawn in the field of the diagram.

On the "cloudy, class 2" diagram (fig. A–2), the minimum temperature lines were drawn from the intersection with the 90 percent relative humidity line to a point of intersection with the 100 percent relative humidity line, corresponding to a dry bulb temperature about 2° higher than the expected minimum temperature line. This was an arbitrary decision, based on the assumption that if the relative humidity were 100 percent at 1730 MST, the dry bulb temperature would only fall about 2° during the night. This decision was based on a few observed cases on foggy nights, but the frequency of such nights in Phoenix is very low so the evidence for determining the configuration of the lines in this region of the chart was flimsy. Physical reasoning would indicate, however, that as the relative humidity approaches 100 percent the release of the latent heat of condensation, as fog formation begins and progresses, should reduce the rate of temperature drop materially, and the minimum temperature lines at high relative humidities should be drawn with that fact in mind. Enough data might be available at coastal stations to do a much better job of analysis in that region of the chart.

Because of the fewer number of cases in the two cloudy categories, the original data sample was extended to include the following years: December 1948–1955; January and February 1949–1956. This gave 175 cases in class 1, and 85 cases in class 2. The verification on original data is shown in table A–1.

The verification on test data was carried out for December 1956, 1957; January and February 1957, 1958 (a total of 64 cases for class 1 and 21 cases for class 2). Because of the scarcity of cases, the verification in table A–1 is given only for the whole test sample for both the climatological aid and the official forecasts.

The importance of being able to forecast cloudiness during the night is especially apparent in the great differences in skill between the climatological aid and the official forecasts for class 2, since the former essentially "knew" the ensuing sky conditions at the time of "forecast."

TABLE A–1.—*Average absolute error for cloudy cases using original data and comparison with official forecasts using test data*

Month	Years used	Original data				Test data					
		Class 1		Class 2		Class 1			Class 2		
		No. cases	Avg. abs. error	No. cases	Avg. abs. error	No. cases	T_o vs. Tw	Off. forecasts	No. cases	T_o vs. Tw	Off. forecasts
Dec.	48–55	56	3.0	28	2.3	64	3.0	3.7	21	3.6	6.4
Jan.	49–56	65	3.0	36	2.5						
Feb.	49–56	54	3.1	21	2.6						
Average		175	3.0	85	2.5						

REFERENCES

1. D. Brunt, *Physical and Dynamical Meteorology*, Cambridge University Press, London, 2nd ed., 1939, pp. 136–142.
2. W. J. Dixon and F. J. Massey, Jr., *Introduction to Statistical Analysis*, McGraw-Hill Book Co. Inc., New York, 1st ed., 1951 (see p. 231).
3. E. S. Ellison, "A Critique on the Construction and Use of Minimum-Temperature Formulas," *Monthly Weather Review*, vol. 56, No. 12, Dec. 1928, pp. 485–495.
4. M. Ezekiel, *Methods of Correlation Analysis*, John Wiley and Sons, Inc., New York, 2nd ed., 1941 (see Chapter 21).
5. W. C. Jacobs, "Application of Brunt's Radiation Equation to Minimum Temperature Forecasting," *Monthly Weather Review*, vol. 67, No. 12, Dec. 1939, pp. 439–443.
6. W. C. Jacobs, "A Convenient Minimum Temperature Diagram," *Bulletin of the American Meteorological Society*, vol. 21, No. 7, Sept. 1940, pp. 297–301.
7. R. K. Linsley, M. A. Kohler, J. L. H. Paulhus, *Applied Hydrology*, McGraw-Hill Book Co. Inc., New York, 1949 (pp. 645–655).

8. E. S. Nichols, "Predicting Minimum Temperatures, Especially as a Function of Preceding Temperature," *Monthly Weather Review*, vol. 58, No. 5, May 1930, pp. 179–189.
9. H. A. Panofsky and G. W. Brier, *Some Applications of Statistics to Meteorology*, Pennsylvania State University, 1958 (see pp. 186–188).
10. W. J. Smith, "Predicting Minimum Temperatures from Hygrometric Data," *Monthly Weather Review, Supplement* No. 16, 1920, pp. 6–19.
11. V. E. Suomi and P. M. Kuhn, "An Economical Net Radiometer," *Tellus*, vol. X, No. 1, 1958, pp. 160–163.
12. F. D. Young, "Forecasting Minimum Temperatures in Oregon and California," *Monthly Weather Review, Supplement* No. 16, 1920, pp. 53–58.
13. N. T. Zikeev, "Selective Annotated Bibliography on Frost and Frost Forecasting," *Meteorological Abstracts and Bibliography*, vol. 4, No. 3, American Meteorological Society, March 1953, pp. 337–397.

SOLAR ENERGY AND SUNSHINE HOURS AT ATHENS, GREECE

GEORGE JAC. MACRIS

National Observatory of Athens, Greece

[Manuscript received November 3, 1958; revised December 15, 1958]

1. INTRODUCTION

Measurements of solar radiation at the earth's surface are restricted to widely scattered locations and in many cases represent relatively short periods of record. Measurements of the hours of sunshine, on the other hand, are more extensive in both time and space.

A number of investigators have successfully applied various forms of the linear relationship between the total daily amount of solar radiation incident on a horizontal surface and the hours of sunshine as proposed by Ångström [1]. This relationship may be expressed as follows:

$$\frac{Q}{Q_0}=a+b\frac{S}{S_0}$$

where Q=total amount of solar radiation impinging on a horizontal square centimeter at the earth's surface per day (expressed in ly. per day).

Q_0=maximum total amount of solar radiation impinging on a horizontal square centimeter at the earth's surface on a perfectly clear day (ly. per day).

S=number of hours of sunshine measured on a sunshine recorder.

S_0=maximum number of hours of sunshine recorded under perfectly clear conditions.

a and b are constants.

The application of such a formula makes it possible to make a quantitative estimate of solar radiation amounts in cases where only the more common sunshine measurements have been made. For example, at Athens, Greece the record of sunshine hours extends from 1901 to the present, while solar radiation measurements have been made only during the last few years [1] [12]. Thus the linear relationship cited above can be used to extend the estimate of solar radiation and its frequency distribution over a far longer period than actual records cover.

2. INSTRUMENTS

At the National Observatory, Athens, Greece [12] daily totals of solar radiation are measured by a Gorczinsky pyrheliometer (No. 111, Richard). For comparison a Kipp and Zonen Solarimeter (No. 604) is used. The number of hours of sunshine is recorded by a Campbell-Stokes Sunshine Recorder. Four years of simultaneous measurements of Q and S, 1953 through 1956, are included in this study.

[1] Some earlier investigations of solar energy at Athens, Greece were reported by Karapiperis [10].

3. CALCULATION OF THE LINEAR RELATIONSHIP

Daily values of $\frac{Q}{Q_0}$ versus $\frac{S}{S_0}$ were plotted for each month and the linear equation for each month was determined by the method of least squares. Examples of such scatter diagrams for the months of March and August are shown in figures 1 and 2.

A lack of scatter in the data for the months of June, July, and August, due to persistent clear conditions made the resulting linear relationships for these months of doubtful value. This difficulty was overcome by approximating the monthly values of b by the average value of b for the other nine months.

4. RESULTS

The monthly values of the constants a and b determined in the above manner are given in table 1. These values give an average of a=.34 and b=.63. These compare with the values found by Fritz and MacDonald [4] for the United States of a=.35 and b=.61.

The variation from month to month of a and b and the variation from location to location in annual values of

TABLE 1.—*Monthly values of solar energy (Q_0 and Q/Q_0), sunshine (S_0 and S/S_0), and linear regression coefficients (a and b) of Q/Q_0 vs S/S_0, Athens, Greece, 1953–56. Q_0 is in ly./day, S_0 in hours/day*

Month	Energy		Sunshine		Intercept a	Linear Slope b
	Q_0	Q/Q_0	S_0	S/S_0		
January	283	.65	9.6	.43	.39	.60
February	365	.72	10.4	.49	.39	.67
March	559	.61	11.5	.50	.29	.65
April	565	.83	12.3	.67	.37	.68
May	628	.83	13.2	.77	.34	.63
June	701	.84	14.2	.87	.29	.63
July	689	.89	14.2	.96	.29	.63
August	656	.85	13.0	.96	.25	.63
September	584	.78	12.5	.80	.32	.58
October	436	.67	10.9	.62	.30	.60
November	277	.74	9.4	.52	.41	.64
December	226	.76	8.6	.55	.44	.58

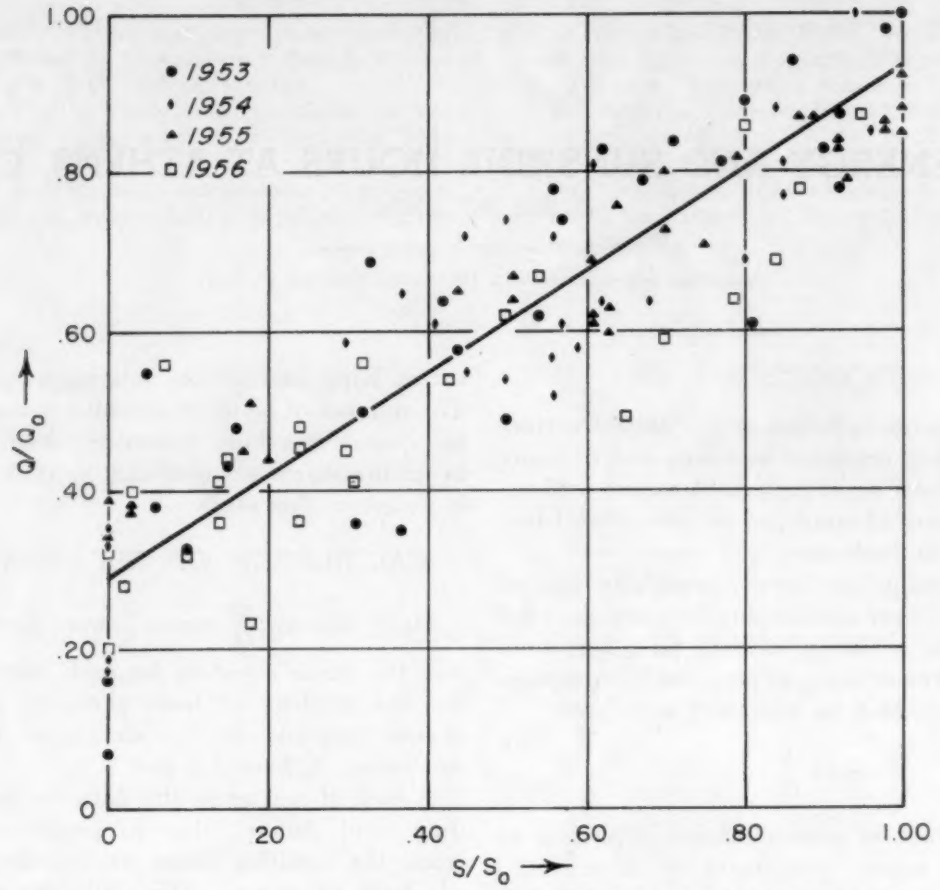

FIGURE 1.—Scatter diagram and linear regression line of Q/Q_0 vs S/S_0 for March, 1953–1956, Athens, Greece.

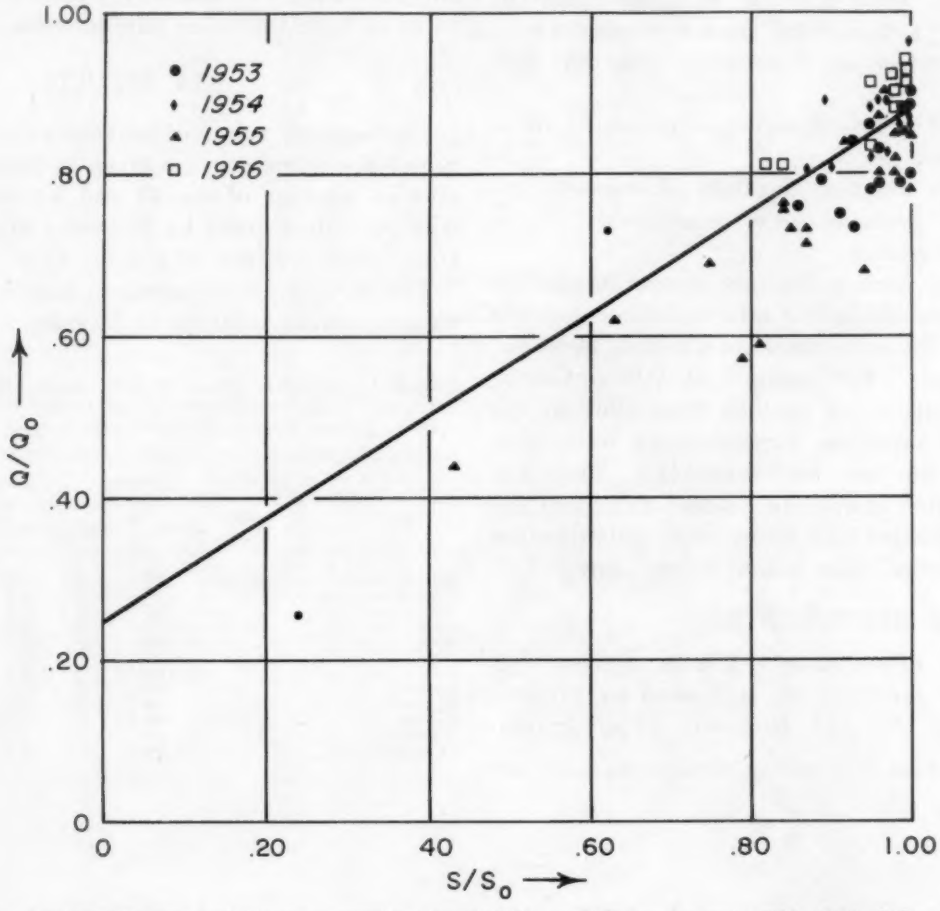

FIGURE 2.—Scatter diagram and linear regression line of Q/Q_0 vs S/S_0 for August, 1953–1956, Athens, Greece.

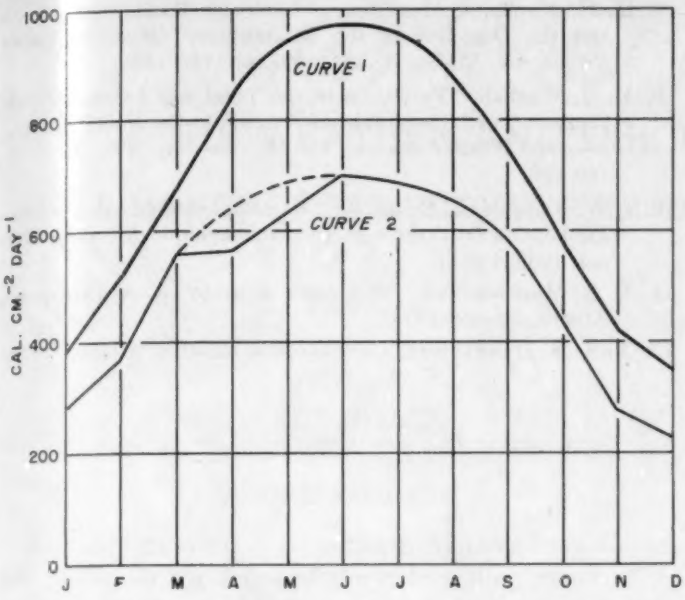

FIGURE 3.—Annual march of solar insolation at top of atmosphere at latitude of Athens, Greece (curve 1). Annual march of maximum solar insolation possible at surface on clear days at latitude of Athens, Greece (curve 2).

these constants are discussed by Ångström [2], Fritz and MacDonald [4], Fritz [5], Kimball [8], [9] and others [6], [7]. Of particular importance in this case are marked seasonal variations in the physical characteristics and distribution of clouds.

Table 1 also contains monthly values of S_o and Q_o as determined from the examination of the maximum perfectly clear day values of S and Q recorded during each month during the period of record.

5. DEPLETION OF SOLAR ENERGY BY THE ATMOSPHERE

Curve 1 of figure 3 is the plot of average daily totals of solar radiation outside the atmosphere at the latitude of Athens, from data by Bernhardt and Philipps [3]. This may be compared with curve 2, a plot of S_o, to illustrate the monthly variation in the depletion of solar radiation by a "clear" atmosphere. The atmosphere is clearer and also drier during the fall and winter than in the summer.

During the months of April and May, the radiation at the surface is lower than expected as curve 2 indicates. This may be due to the additional absorption of solar energy by water vapor in the moist air masses which move off the Mediterranean from the southwest, and which are prevalent in these two months. In other months of the year the prevailing winds are northeasterly [11] and the water vapor content of the atmosphere is much lower.

6. FREQUENCY DISTRIBUTIONS OF TOTAL HOURS OF SUNSHINE

Frequency distribution histograms of the total hours of sunshine were determined for Athens on the basis of records from 1901 until 1956. Two examples of these histograms from 1953 to 1956 are illustrated in figures 4 and 5. Of particular importance is the frequent occurrence of clear days during the summer months. In July 87 percent of the days have more than 13 hours of sunshine. This is in sharp contrast with the more nearly uniform distribution of the winter months with January showing 20 percent of its days with less than one hour of sunshine.

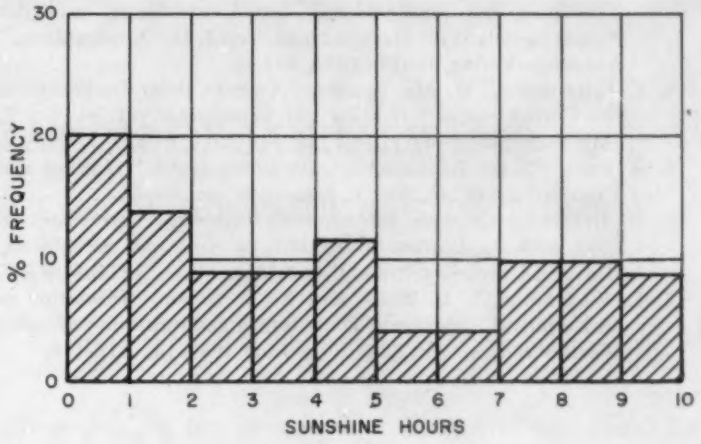

FIGURE 4.—Histogram of total hours of sunshine for January, 1953–1956, Athens, Greece.

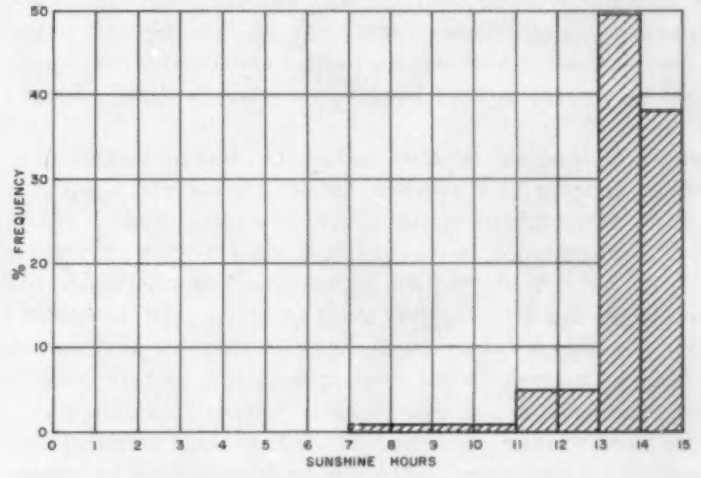

FIGURE 5.—Histogram of total hours of sunshine for July, 1953–1956, Athens, Greece.

REFERENCES

1. A. Ångström, "Solar and Terrestrial Radiation," *Quarterly Journal of the Royal Meteorological Society*, vol. 50, No. 210, Apr. 1924, pp. 121–125.
2. A. Ångström, "On the Computation of Global Radiation from Records of Sunshine," *Arkiv för Geofysik*, Band 2, Hefte 5, Nr. 22, 1956, pp. 471–479.
3. F. Bernhardt and H. Philipps, "Die Räumliche und Zeitliche

Verteilung der Einstrahlung, der Ausstrahlung, und der Strahlungsbilanz im Meeresniveau, Teil 1, Die Einstrahlung," Academie-Verlag, Berlin, 1958, 227 pp.

4. S. Fritz and T. H. MacDonald, "Average Solar Radiation in the United States," *Heating and Ventilating*, vol. 46, No. 7, July 1949, pp. 61–64.
5. S. Fritz, "Solar Radiation on Cloudless Days," *Heating and Ventilating*, vol. 46, No. 1, Jan. 1949, pp. 69–74.
6. B. Haurwitz, *Daytime Radiation at Blue Hill Observatory in 1933, with Application to Turbidity in American Air Masses*, Harvard University Press, Cambridge, Mass., 1934, 31 pp.
7. R. W. Hamon, L. L. Weiss, and W. T. Wilson, "Insolation as an Empirical Function of Daily Sunshine Duration," *Monthly Weather Review*, vol. 82, No. 6, June 1954, pp. 141–146.
8. H. H. Kimball, "Measurements of Solar Radiation Intensity and the Depletion of the Atmosphere," *Monthly Weather Review*, vol. 55, No. 4, Apr. 1927, pp. 155–169.
9. H. H. Kimball, "Variations in the Total and Luminous Solar Radiation with Geographical Position in the United States," *Monthly Weather Review*, vol. 47, No. 11, Nov. 1919, pp. 769–793.
10. L. N. Karapiperis, *Recherches sur la Radiation solaire à Athènes*, Publication de l'Observatoire Astronomique Royale d'Athènes, 1939, 131 pp.
11. E. G. Mariolopoulos, *The Climate of Greece*, A. A. Papaspyros, Athens, Greece, 1938.
12. National Observatory, *Climatological Bulletin*, Athens, Greece.

THE WEATHER AND CIRCULATION OF JANUARY 1959

A MONTH OF EXCEPTIONAL PERSISTENCE FROM THE PRECEDING DECEMBER

L. P. STARK

Extended Forecast Section, U.S. Weather Bureau, Washington, D.C.

1. PERSISTENCE FROM DECEMBER 1958 TO JANUARY 1959

WEATHER ANOMALIES

Very high persistence over North America from December to January was one of the outstanding facets of the monthly mean weather and circulation of January 1959. One should anticipate a normal increase in month-to-month persistence of temperature, mean 700-mb. heights, and to a lesser degree, precipitation in passing from fall into winter [1]. However, stability of pattern and weather anomalies from December to January was so great this year that special emphasis is warranted.

Class changes of monthly mean temperature in the United States are shown in table 1. These data were derived from an array of 100 well-distributed stations and represent changes in classes based on the normal distribution of temperature at each city. The classes much above and much below normally occur 12½ percent of the time each, and above, normal, and below normally occur 25 percent of the time each. On examining the table, one is first struck by the absence of any change exceeding two classes. But even more significant, and certainly more indicative of the month's persistence, is the fact that 96 percent of the stations did not change by more than one class.

It is interesting to compare the results in table 1 with the averages determined by Namias [1] for the period 1942–1954. In his study the average number of 0+1 class changes (no change or a change of one class) for December to January was 71 percent. By comparison, January 1959 with 96 percent was phenomenally static. Fairly high persistence has been found in other Januarys (e.g., 1956 [2]), but in the last 17 years there has not been a January with smaller temperature changes than this year. Parenthetically, it should be noted that 0+1 class temperature persistence greater than 90 percent has been observed only 17 times since April 1942 (8 percent of the time).

Precipitation from December 1958 to January 1959 was also quite persistent. Table 1 shows a 47 percent value of the 0 class change in precipitation for January. This represents rather high stability when compared to the December-January average of 37 percent for the years 1942–1954 [1]. In fact, there were only three previous Januarys in the past 17 years in which the 0 class change of precipitation was greater than the 47 percent of 1959.

It is difficult to make direct comparison of persistence of precipitation with that of temperature since values are computed for 0 class change for the former and 0+1 class change for the latter. However, the two can be compared by expressing them in terms of their long-period average. For example, this month's persistence of precipitation was 127 percent of the 13-year average value, while the corresponding figure for temperature was 135 percent.

TABLE 1.—*Class changes of weather anomalies in the United States from December 1958 to January 1959*

Class Change	Frequency (percent)
Temperature	
0	54
1	42
2	4
3	0
4	0
Precipitation	
0	47
1	35
2	18

CIRCULATION

Persistence of the 700-mb. pattern was as pronounced as that of the weather anomalies. A qualitative comparison of the 30-day mean 700-mb. chart for January 1959 (fig. 1) with that of December 1958 (fig. 1 of [3]) shows a ridge in western North America, a trough along the east coast, and a Low in Canada. Height departures from normal in the same figures show a remarkable similarity.

A quantitative evaluation of circulation persistence can be expressed in terms of a lag correlation between the patterns of height anomalies. This was done earlier [1] for the period 1933–1950, using a grid extending from 30° to 50° N. and from 70° to 130° W. An average lag correlation of +0.36 was obtained for all December to January periods. A similar correlation computed for Decem-

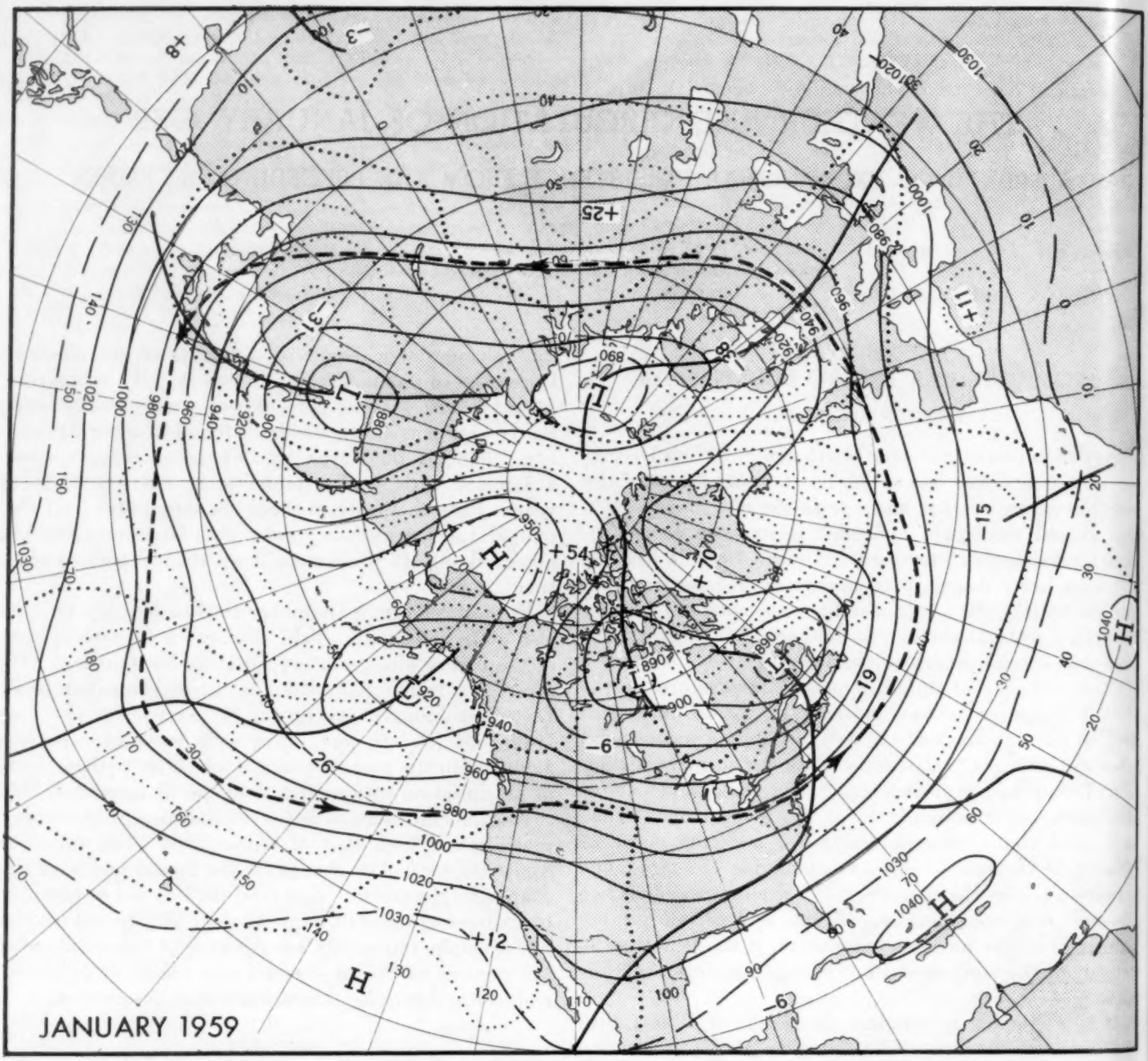

FIGURE 1.—Mean 700-mb. contours (solid) and height departures from normal (dotted) (both in tens of feet) for January 1959. Heavy dashed arrows represent the axis of the mean 700-mb. wind maximum. Widespread positive height departures over the polar region reflected intense blocking there.

ber 1958 to January 1959 was +0.61, substantially greater than the average for the 18-year period above.

There was one feature of the circulation not wholly consistent with the high persistence. A marked change occurred in the strength of the 700-mb. temperate westerlies (35°–55° N., computed twice monthly for overlapping 30-day periods). The zonal index for the western half of the Northern Hemisphere for December was 12 m.p.s., 0.7 m.p.s. above normal. During January the index decreased to 9.9 m.p.s., 1.9 m.p.s. below normal. This is the first month in the last nine in which the temperate index averaged below normal. The value of the 30-day mean sea level index in temperate latitudes averaged 1.6 m.p.s. below normal, following a near normal index in December. The configuration of systems typical of low index can be seen on the 30-day mean sea level chart (fig. 2). These features include split Aleutian and Icelandic Lows, strong polar Highs, and weak subtropical Highs.

2. MAJOR FEATURES OF THE NORTHERN HEMISPHERE CIRCULATION

The hemispheric circulation in January 1959 (fig. 1) consisted of a wave number of four in middle latitudes.

The troughs at higher latitudes in the western half of the Northern Hemisphere were rather weak compared with those of the eastern half. This is shown by the relative intensity of the 700-mb. 30-day mean height departures from normal. The troughs near North America were less intense and did not penetrate as far northward as did those of Europe and Asia.

The circulation in midtroposphere in far northern latitudes of the Western Hemisphere was much more anticyclonic than that which normally prevails [4]. The large High over the Beaufort Sea was an especially significant center of action in influencing weather in the United States. It was part of a very extensive band of positive height anomalies which blanketed the area from the Bering Sea to Denmark Strait with heights ranging from 400 to 700 feet above normal. The unusual circulation in that region, which included anomalous centers of the greatest absolute magnitude in figure 1 and which dominated the flow in the Northern Hemisphere, was also conspicuous in the weather and circulation regime of December. In fact, high-latitude blocking over North America has been a circulation feature of varying magnitude in each month since June 1958.

A fairly well-developed Low in the Gulf of Alaska and its attendant trough south-southwestward maintained the approximate intensity observed in December (fig. 1 of [3]), but important changes occurred. The trough acquired a positive tilt as the lower portion retrograded some 25° from its December position. As the trough along the coast of Asia deepened, the wavelength in the Pacific shortened. The fast westerlies observed in mid-Pacific in December were replaced by a difluent zone near the International Date Line, and the mean 700-mb. wind speed maximum (shown by a dashed arrow in fig. 1) was displaced 10° southward in January from its position near 37° N. in December (see fig. 3A of [3]).

Though the ridge-trough couplet over the United States and Canada appears to have been of small amplitude, the flow was vigorous enough to keep the West warm and the rest of the United States quite cold (fig. 3). The 30-day mean 700–1000-mb. thickness anomaly field (fig. 4) shows the extent of the cold air and its extremely cold pool over northern British Columbia. The channel of cold air from northwestern Canada to Tennessee was practically coincident with a strong ridge of high pressure at sea level (fig. 2) and with the path of maximum anticyclonic activity, illustrated in figure 2 as a heavy dashed arrow. (See also tracks of centers of anticyclones at sea level, Chart IX, of [5].)

The ridge over Greenland, principally a development of the first half of the month, was closely associated with the strength of the trough in Europe. The westerly flow into central Europe met the northwesterly flow from the Arctic in a zone of strong confluence, and cold air was thus contained north of 50° N. in the mean (see fig. 4).

Strong westerlies across northern Asia, with the axis of the mean 700-mb. wind speed maximum reaching 60° N.

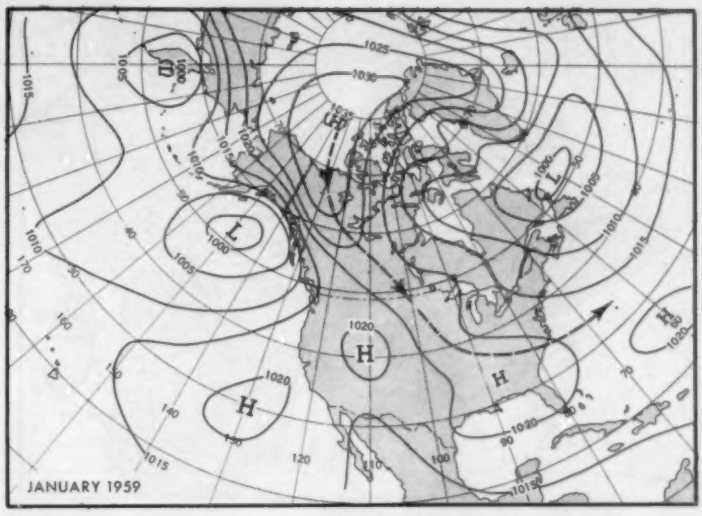

FIGURE 2.—Mean sea level isobars (in millibars) for January 1959. Heavy dashed arrows represent the main anticyclone track in January. The prominent ridge from the Arctic Ocean to the Gulf of Mexico shows the southward drive of cold air.

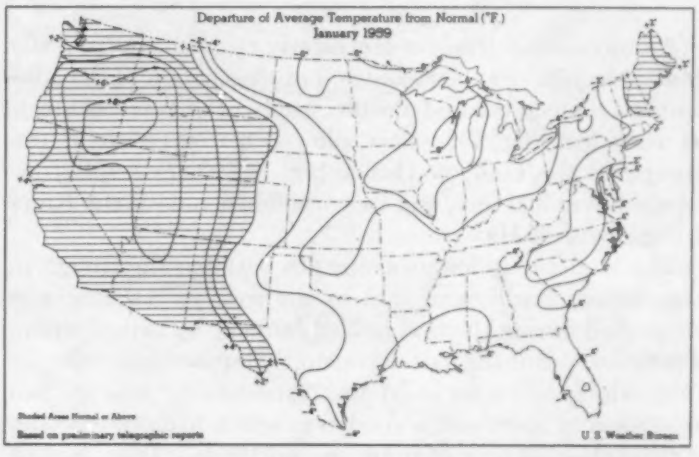

FIGURE 3.—Departure of average temperature from normal (° F.), January 1959. Hatching indicates areas of normal or above normal temperatures. The barrier effect of the Rockies is well shown as cold air stayed east of Divide.

(fig. 1), accommodated the long wavelength downstream to the next trough in eastern Asia. Adequate cold air supported the strong, full-latitude trough observed in that area, which is also a zone of high trough frequency climatologically [6].

3. VARIABILITY IN THE WESTERN HEMISPHERE DURING JANUARY

Since the 30-day mean smooths shorter-term variations in the pattern, a breakdown of the mean into 15-day components is of some interest. It has been noted above that the January pattern closely resembled that of the preceding month. One might thereby reasonably expect persistence within the month. But a comparison of the circulation of the first and last halves of the month (figs. 5 and 6) reveals rather sudden changes.

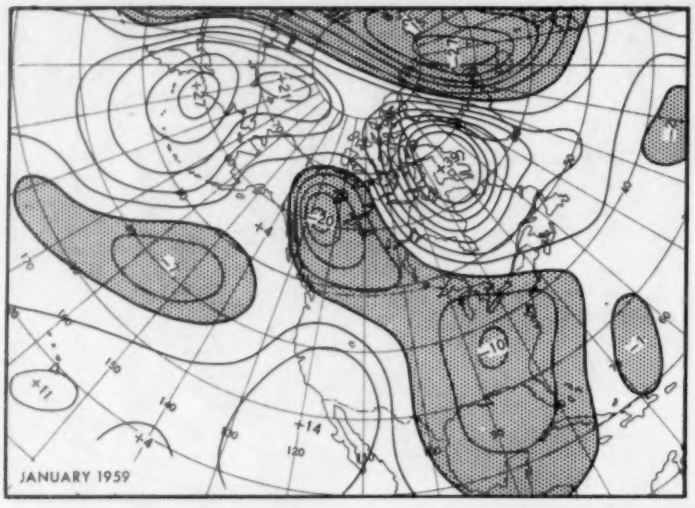

FIGURE 4.—Mean thickness (1000–700 mb.) departures from normal (tens of feet) for January 1959. Below normal thickness areas (shaded) were almost identical to areas of below normal surface temperature (fig. 3).

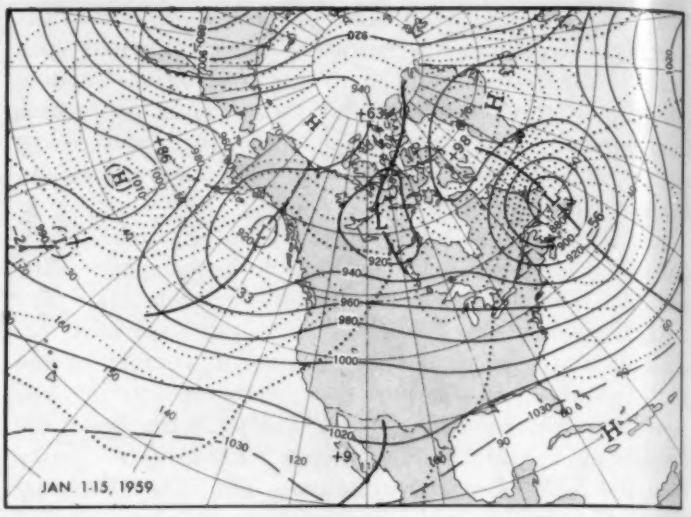

FIGURE 5.—Mean 700-mb. contours (solid) and height departures from normal (dotted) (both in tens of feet) for January 1–15, 1959. Fast westerlies and a long half wavelength dominated the United States.

A downstream transfer of westerly momentum from the coastal trough near Asia assisted in the erosion of the subtropical ridge in the mid-Pacific, where heights fell as much as 1000 feet (fig. 7). This allowed retrogression of the trough in the Gulf of Alaska (fig. 6), where heights increased over 300 feet, and its consolidation with the Kona trough west of Hawaii.

The moderately long wavelength between the trough in the eastern Pacific and that in the western Atlantic was supported during the first half of January by rather strong westerlies. But the half-wavelength downstream from the ridge along the west coast was considerably longer than that usually observed, a condition which usually precedes a circulation change of major proportions. The vigorous new trough over the Mississippi Valley in the succeeding half-month (fig. 6) is an excellent example of a new mean trough development as described by Namias [7] and apparently was associated with:

a. A wavelength too long to be supported by the speed of the westerlies.

b. Retrogression of the ridge in western North America and its intensification as it amalgamated with the Arctic Basin High.

c. Strengthening of the trough in central Canada.

d. Northeastward extension of the trough in Mexico.

This classical development of a new trough is also a prime example of amplification of the contour pattern. The intensity of the change from figure 5 to figure 6 is depicted in figure 7, the change in height anomaly from the first to the last half of January. Meanwhile the trough in the western Atlantic was swept eastward to the Azores, where heights decreased over 400 feet. South of Newfoundland height increases exceeded 700 feet as a strong ridge replaced the trough.

Temperature anomalies for each half of the month, as seen in figure 8 A and B, appear very much alike in spite of differences in circulation. However, an examination of figure 8C shows significant changes related to the evolving circulation. Note especially the negative anomalous temperature change in figure 8C and compare it with the height change in figure 7. Positive height anomalies of January 1–15 were replaced by negative anomalies of January 16–30 from Hudson Bay to the Gulf of Mexico and from the Continental Divide to the Ohio Valley. At the same time, temperature anomalies became more negative in the Plains and Central States as far south as Arkansas. Maximum changes of 10° F. were reported near the Canadian border. Partially as a result of the new trough development, temperatures increased in the South, the Northwest, and the East. An increase of 6° F. occurred in Virginia in advance of the trough.

The decreases of temperature in the Far West are more puzzling. An increase in 700-mb. height anomaly (fig. 7) does not usually imply a decrease in temperature. Many factors could contribute to a cooling, but perhaps most important in this case was the direction of anomalous flow, which changed from southwest the first half of the month to northwest the last 15 days, as the ridge retrograded from the Rocky Mountains to the west coast. However, even though there was considerable intramonthly cooling, mean temperatures were still above normal in the Far West and Southwest for the period January 16–30.

4. WEATHER IN THE UNITED STATES RELATED TO CIRCULATION

TEMPERATURE

Several injections of Arctic air into the United States east of the Divide produced a cold regime in the East.

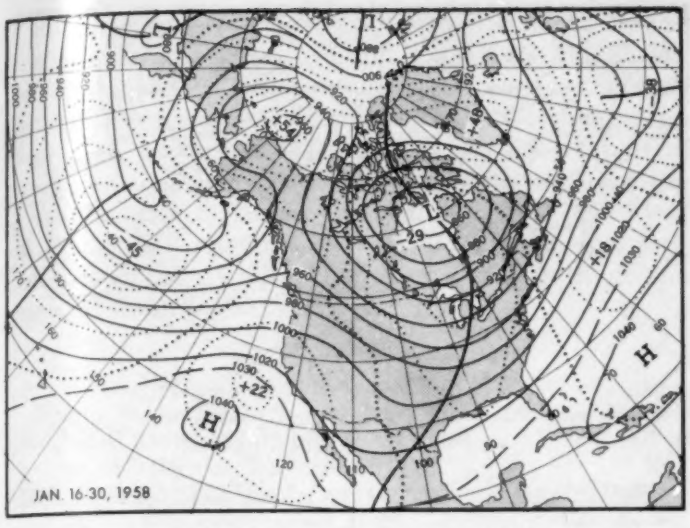

FIGURE 6.—Mean 700-mb. contours (solid) and height departures from normal (dotted) (both in tens of feet) for January 16–30, 1959. Note new trough which formed in central United States as the ridge in the West retrograded and the trough in the western Atlantic progressed.

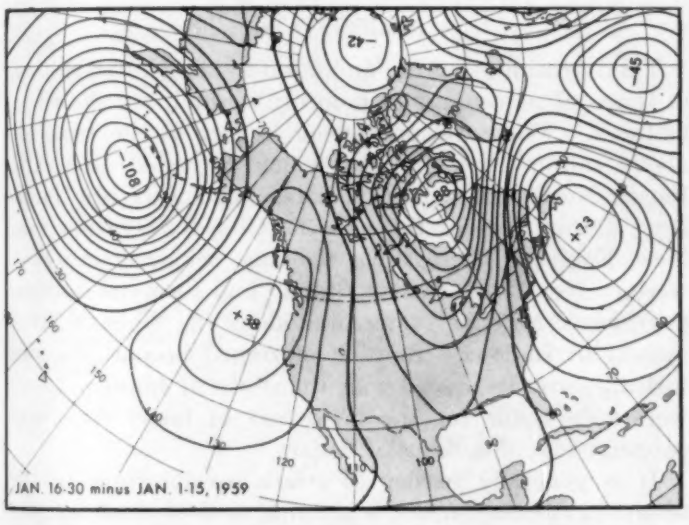

FIGURE 7.—Change of mean 700-mb. height departure from normal (tens of feet) from January 1–15 to January 16–30, 1959. This pattern accompanied considerable amplification of the long waves.

This, together with warming in the West, resulted in a distribution of temperature which was meridional, a situation generally associated with great temperature extremes. In this month, for example, the warmest January of record was observed at Los Angeles and San Francisco, while Muskegon, Mich. and International Falls, Minn. were having the coldest (and snowiest at Muskegon) January of all time.[1]

Extreme cold early in January accompanied a front which dropped daily temperatures as much as 50° and was responsible for a weekly average temperature of 20° below normal at Amarillo, Tex. [8]. As cold air spread to the east coast, warming occurred throughout the West. An example of the magnitude of that change was recorded

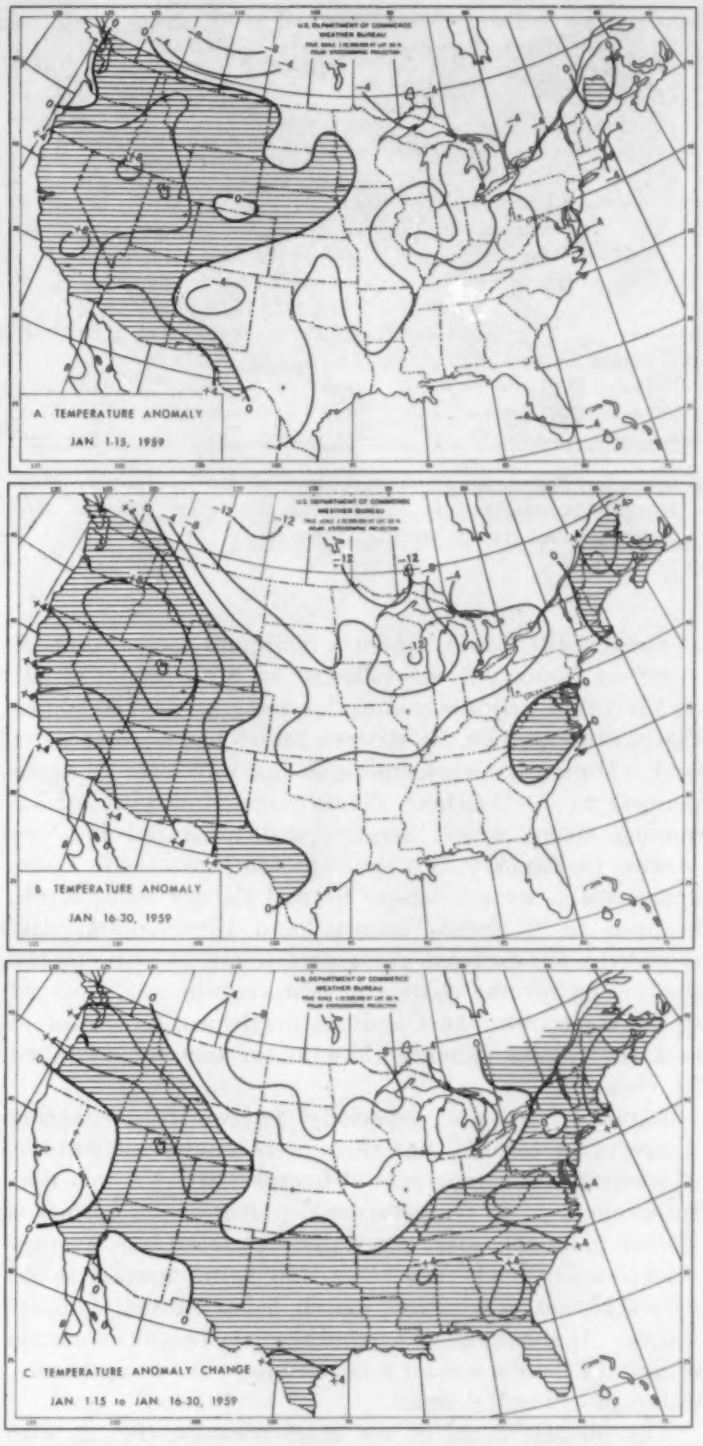

FIGURE 8.—Temperature departure from normal (° F.) for (A) January 1–15, 1959, (B) January 16–31, 1959. Shaded areas are normal or above. In (A) warming east of Divide in Plains States was related to foehn action. In (B) note cooling in North Central and Northern Plains States. (C) Change in temperature departure from normal (° F.) from January 1–15 to January 16–31, 1959. Shaded areas represent positive changes (warming). (From [8].)

[1] From *Local Climatological Data* report of each city, January 1959.

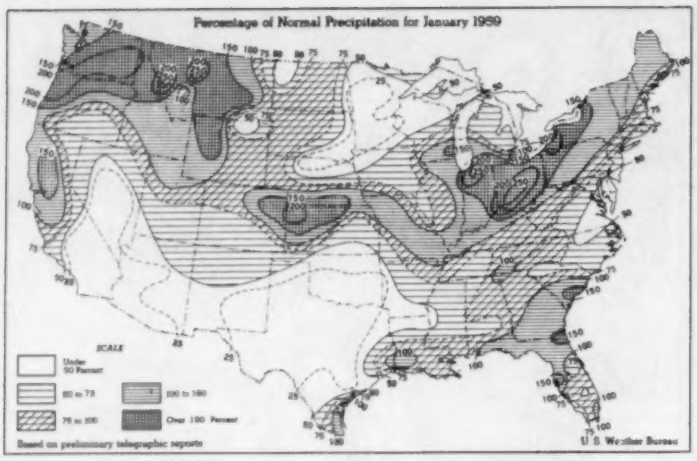

FIGURE 9.—Percentage of normal precipitation for January 1959. Heaviest amounts were found near the mean 700-mb. wind maximum and cyclone track. (From [8].)

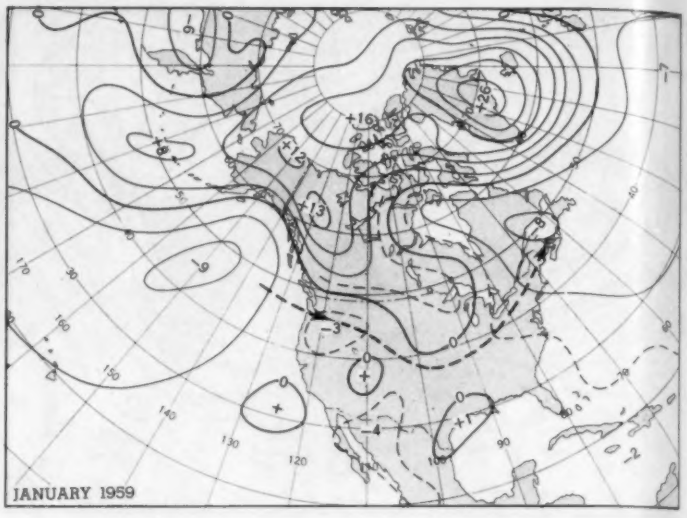

FIGURE 10.—Mean sea level pressure departure from normal (millibars) and principal cyclone track (heavy dashed arrows). There was a close correspondence between the position of the storm track, the mean 700-mb. wind maximum, and area of heavy precipitation.

at Great Falls, Mont. where a minimum temperature of —29° on January 3 was followed by a maximum of 62° on the 12th.[1] By midmonth, warming progressed to the Plains States, while the Eastern States had become quite cold. During the week ending January 25, cold air again plunged to the Southern Plains States, following a fast-moving storm which became well organized in New Mexico on January 20. Average temperatures in Oklahoma, which were 6° above normal the preceding week, dropped to 6° below normal, and Birmingham, Ala. recorded a 52° decrease in temperature in 18 hours on the 21st. The reverse change in temperature was reported in the East from the Carolinas northward and resulted in a spectacular January thaw in the manner described by Wahl [9].

January was not especially noteworthy regarding temperature records, but there were additional features of interest. A comparison of figures 3 and 4 shows that the isopleth of 0° temperature departure from normal is almost identical with the zero isopleth of the average thickness DN. One also sees that below normal thicknesses almost everywhere match below normal temperatures. It should also be noted that the height anomalies of figure 1 have a similar relationship to the temperature, although less well defined.

The 30-day mean of sea level pressure (fig. 2) also helps explain the temperature distribution of figure 3. The ridge from the Beaufort Sea to Florida and the flow from the District of Mackenzie to the Atlantic Coast States defines the source of cold air and its transport southeastward. The warm High over the Great Basin and the onshore flow into the West are indicative of the above normal temperatures observed there. It is of some historical significance that California coastal areas have escaped the below normal category since early April 1958, except for two consecutive 5-day periods in mid-November.

PRECIPITATION

Total precipitation accumulation in the United States, in terms of percentage of monthly normal, are shown in figure 9. The most prominent feature is the band of above normal precipitation which extended from the Pacific Northwest (where Spokane had its wettest January), across Kansas, through the Ohio Valley, and into New England. Disastrous flooding occurred in Ohio, western New York (where Buffalo had its wettest January), western Pennsylvania, and along the Wabash River system in Indiana. Rainfall of record proportions and melting snow associated with the storm of January 20–23 were responsible for the flood loss of many lives and property loss of millions of dollars.

It is generally harder to relate precipitation to the observed circulation or its anomalous flow than temperature. In this January, however, the task is relatively simple. In figure 10, the 30-day mean sea level pressure departures, one can see a corridor of negative values which closely resembles the configuration of the area of heavy precipitation. This was related to the principal storm track during January, represented by the heavy dashed arrow. The storm track is based on an analysis of frequencies of cyclones in a grid of equal area boxes and on inspection of tracks of daily centers of cyclones at sea level (Chart X of [5]). Note also the proximity of the 700-mb. mean wind speed maximum (in fig. 1) to the cyclone track and axis of heavy precipitation. Compared with normal tracks and mean frequencies of cyclones [10], those in January were displaced southward 5°–10° of latitude, presumably as a consequence of high-latitude blocking and the resultant depression of the westerlies.

Referring again to figure 9, other areas of above normal precipitation are shown in California, where Mt. Shasta had the wettest January since 1916. There was a secondary streak from northern Texas to South Carolina. The large area which had less than 50 percent of normal precipitation included Dallas, Tex., which reported the driest January of record, and Albuquerque, N. Mex. which reported its sunniest. Dry weather in this area was related to northwesterly flow aloft south of the principal storm track.

REFERENCES

1. J. Namias, "The Annual Course of Month-to-Month Persistence in Climatic Anomalies," *Bulletin of the American Meteorological Society*, vol. 33, No. 7, Sept, 1952, pp. 279–285, and an unpublished extension through 1954.
2. W. H. Klein, "The Weather and Circulation of January 1956—A Month with a Record Low Index," *Monthly Weather Review*, vol. 84, No. 1, Jan. 1956, pp. 25–34.
3. R. A. Green, "The Weather and Circulation of December 1958," *Monthly Weather Review*, vol. 86, No. 12, Dec. 1958, pp. 487–492.
4. U.S. Weather Bureau, "Normal Weather Charts for the Northern Hemisphere," *Technical Paper* No. 21, 1952, 74 pp.
5. U.S. Weather Bureau, *Climatological Data, National Summary*, vol. 10, No. 1, Jan. 1959.
6. W. H. Klein and J. S. Winston, "Geographical Frequency of Troughs and Ridges on Mean 700-mb. Charts," *Monthly Weather Review*, vol. 86, No. 9, Sept. 1958, pp. 344–358.
7. J. Namias, *Extended Forecasting by Mean Circulation Methods*, U.S. Weather Bureau, Feb. 1947, 89 pp.
8. U.S. Weather Bureau, *Weekly Weather and Crop Bulletin, National Summary*, vol. XLVI, No. 1, Jan. 5, 1959, and No. 8, Feb. 23, 1959.
9. E. Wahl, "The January Thaw in New England," *Bulletin of the American Meteorological Society*, vol. 33, No. 9, Nov. 1952, pp. 380–386.
10. W. H. Klein, "Principal Tracks and Mean Frequencies of Cyclones and Anticyclones in the Northern Hemisphere," U.S. Weather Bureau, *Research Paper* No. 40, 1957, 40 pp.

Weather Note

TORNADOES OF JANUARY 21, 1959—A FEATURE OF A WEATHER SINGULARITY?

ROBERT R. DICKSON

U.S. Weather Bureau, Nashville, Tenn.

[Manuscript received February 2, 1959]

ABSTRACT

The tornadoes of January 21, 1959, in Tennessee and neighboring States are considered in relation to the New England January thaw singularity described by Wahl [1]. This singularity, in the form of a warm spell, is shown to occur on the average on January 20–22 at Nashville. It is shown that at the time of the singularity there coexist on the average in the Tennessee area certain conditions favorable for the formation of severe storms. These include a tongue of warm, moist air at the surface, a wind shift from southerlies during the warm period to cool northwesterlies immediately afterward, a 500-mb. trough to the west with southwesterly winds and contour inflection point over the Tennessee area, and the presence of a jet stream aloft. Review of past records reveals that tornadoes in the Arkansas, Alabama, Mississippi, Tennessee, and Kentucky area have occurred more often during the time of the singularity, January 20–22, than at any other time of the month.

1. INTRODUCTION

On January 18, 1959, surface winds from the Gulf Coast northward to the Great Lakes shifted to southerly quadrants, heralding the end of the existing cold spell. From Kentucky southward this warming continued through the morning of January 21, culminating in temperatures of 70° F. or higher over most of the Southeast. The surface weather system responsible for the final northward surge of warm, moist air was an intense open wave on the polar front which moved rapidly from central Texas to near Detroit by 0000 GMT, January 22. As the associated cold front swept across the Southeast displacing maritime tropical air, a series of severe thunderstorms and tornadoes broke out. Preliminary reports placed tornado activity in Mississippi, Alabama, Tennessee, and Kentucky. As the tornado-spawning Low moved northeastward, 60° F. temperatures reached northward to Boston prior to the cold front passage near noon on January 22.

2. THE NEW ENGLAND JANUARY THAW SINGULARITY

The advent of 60° F. temperatures in the Boston area on January 22, 1959, occurred at precisely the period (January 20–23) of the New England January thaw singularity described by Wahl [1]. Compared with the normal January daily maximum temperature at Boston of 36.5° F., this January 22 warming constituted an exceedingly well-developed example of the singularity.

Wahl discussed the validity of the January thaw singularity for the eastern portion of the United States, using data for the Boston, New York, Washington, D.C., and Columbia, Mo., areas. Evidence of this singularity in Tennessee may be found in figure 1a. Mean daily temperature at Nashville, averaged over the period 1871–1950 [2], shows an increase to 41.9° F. on January 21—nearly 3° warmer than the average temperature 2 days before or 3 days after that date. Thus the Tennessee counterpart of the New England January thaw singularity is established as occurring on January 20–22.

3. SYNOPTIC IMPLICATIONS

Wahl [1] illustrates the remarkable extent to which the singularity shows up in 40-year average sea level pressure patterns. His figure 4b shows the existence of warming southerly winds on January 20 from the Gulf of Mexico to New England, accompanying the warm-spell singularity on January 20–22 at Nashville and January 20–23 in New England. By January 27, as indicated in his figure 4c, the warm air over the eastern half of the country has been swept away by a cold High from the northwest. Figures 1b

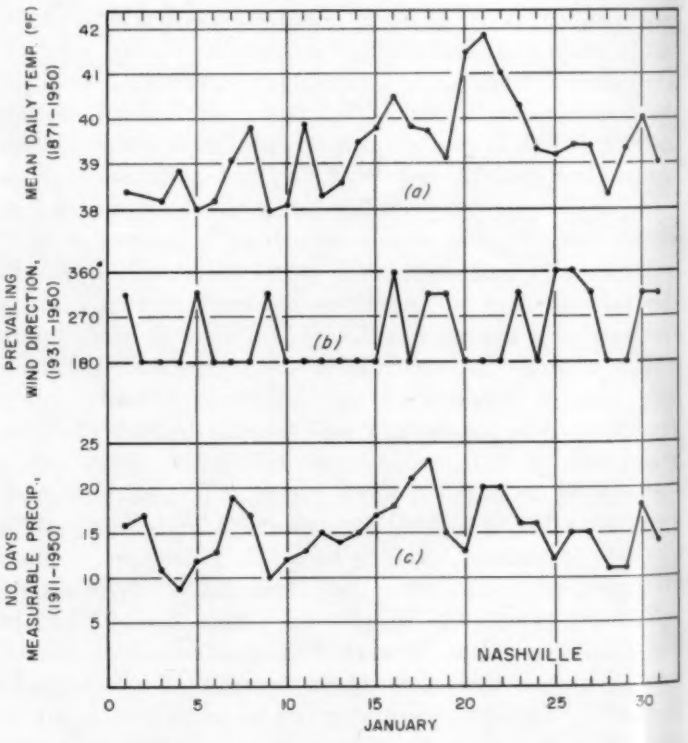

FIGURE 1.—Data for Nashville, Tenn. (a) Daily average temperature, 1871–1950; (b) Prevailing wind direction, 1931–1950; (c) Frequency of days with measurable precipitation, 1911–1950.

and 1c serve to document this sequence of events further. Prevailing wind at Nashville [3] is from the south on January 20–22 giving way to northwesterly winds on January 23, thus suggesting a cold front passage. It is of interest to note that on January 21 prevailing winds at Nashville are from the quadrant SW–SE 70 percent of the time. Figure 1c shows a secondary maximum in the frequency of days with measurable precipitation at Nashville [3] on January 21 and 22 accompanying the wind shift described above.

To further assay the potential of the synoptic situation associated with the January 20–22 warm-spell singularity, the concurrent upper-level circulation was investigated. Figures 2 and 3 are 500-mb. mean charts and their departures from normal for January 20 and January 27 respectively for 1948–1957 (1955 missing). The 500-mb. trough on January 20 stretches from western Texas northward to the Great Lakes, a position near the January normal. However, the anomaly lines show that the southern portion of the trough is deeper than normal and winds over the eastern part of the country are more southerly than the January normal. Attention is also directed to the location of the 18,400-ft. contour on January 20 in the Arkansas, Kentucky, Tennessee area. As pointed out by Fletcher [4] the axis of maximum wind at 500 mb. is most frequently associated with the 18,400-ft. contour and is within the contour range 18,200–18,800 ft. 91.8 percent of the time. Since experience verifies a reasonably close identity between the location of the axis of maximum wind at 500 mb. and the jet stream core over the eastern United States, the jet stream on January 20 (fig. 2) can be considered to cross the Arkansas-Kentucky-Tennessee area near the 18,400-foot contour.

Figure 3 illustrates the eastward progression, shear, and decrease in intensity of the mean trough in central United States by January 27. Height change from the January 20 average map of figure 2 to the January 27 average map of figure 3 is shown in figure 4. The difference between these average daily 500-mb. charts one week apart is striking.

As shown by the long-term average circulation at both sea level and 500 mb., some of the necessary conditions for the generation of severe storms in the general area exist at the time of the January 20–22 warm-spell singularity in Tennessee. A surface tongue of warm (and by inference moist) air, introduced by persistent south winds, stretches from the Gulf through Tennessee to New England. This tongue of warm, moist air is subsequently displaced by cold air which brings a notable temperature drop and shifts surface winds from the south to the northwest in the Tennessee area. Aloft, a 500-mb. trough, deeper than normal in southern portions, lies immediately to the west, with southwesterly flow and contour inflection point over the Tennessee area. Furthermore, the axis of the jet stream, as deduced from 500-mb. contours, traverses the area.

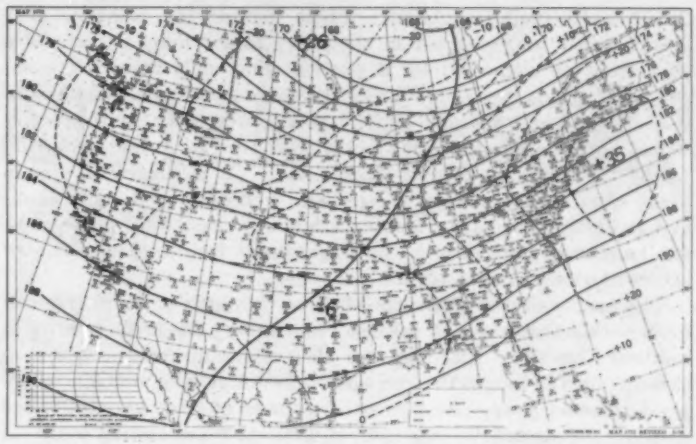

FIGURE 2.—500-mb. mean map for January 20, 1948–1957 (less 1955). Height contours (100's of feet) are solid lines, departures from normal (10's of feet) are dashed lines.

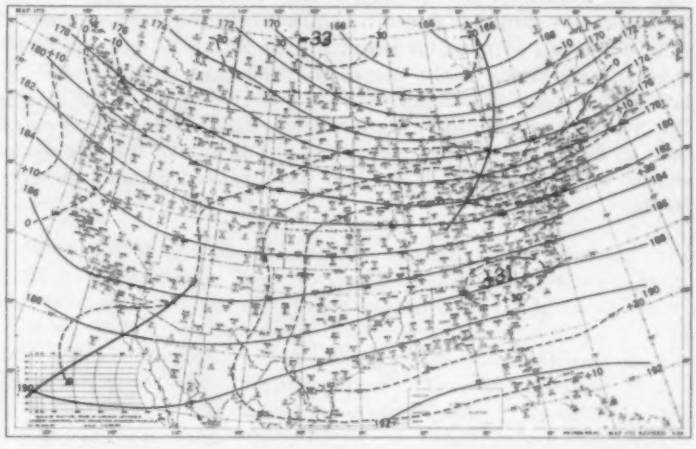

FIGURE 3.—500-mb. mean map for January 27, 1948–1957 (less 1955). Height contours (100's of feet) are solid lines, departures from normal (10's of feet) are dashed lines.

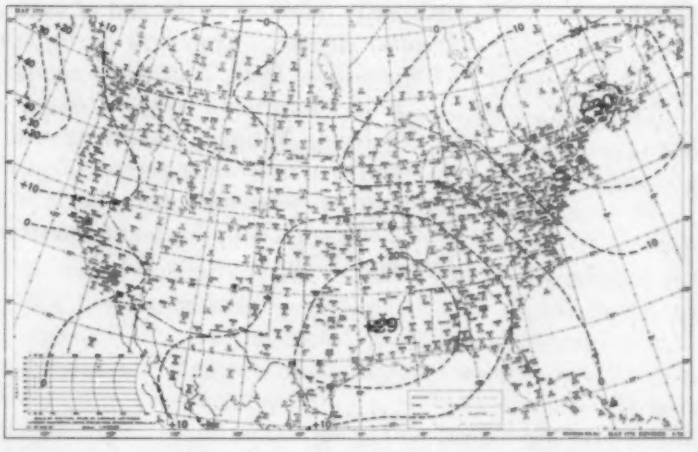

FIGURE 4.—500-mb. height change (10's of feet) from January 20 mean map (fig. 2) to that of January 27 (fig. 3).

4. TORNADO DISTRIBUTION IN JANUARY

A search of past records from 1931 through 1959 for the Alabama, Mississippi, Arkansas, Tennessee, Kentucky area [5] reveals a total of 28 tornado days during the month of January. Of these, six (21 percent) occurred from January 20–22 in association with the singularity under consideration. A similar concentration of tornado occurrence is found in only one other January period, January 29–31, when six tornado days have been observed. The number of tornadoes on any January day for the 1931–1958 period reaches a maximum of 12 on January 22 and does not exceed 5 on any other January day. Furthermore, preliminary, unverified reports indicate that 11 tornadoes occurred on January 21, 1959, to give a preponderance of January tornadoes during the January 20–22 warm-spell singularity.

5. CONCLUSIONS

Long-term average temperature data for Nashville give evidence in the Tennessee area of a warm-spell singularity on January 20–22—possibly the Tennessee counterpart of the New England January thaw singularity described by Wahl [1]. Examination of average circulation features at sea level and the 500-mb. level reveals the existence of certain conditions favorable for the development of severe storms in the Tennessee area at the time of the January

20–22 warm-spell singularity. These include the presence of a warm, moist tongue of air in the lower atmosphere, passage of a cold front as suggested by a surface wind shift from persistent southerly winds prevalent during the warm spell to cooling northwesterly winds, a 500-mb. trough to the west with southwesterly winds and contour inflection point over the Tennessee area, and finally the presence of a jet stream aloft. It is suggested that in years when the singularity is especially well developed, as in January 1959, the singularity and its attendant circulation patterns at sea level and aloft provide the ingredients for the generation of severe storms in Tennessee and vicinity.

The results of this study are of value primarily as another bit of evidence dealing with the validity of a January 20–22 singularity in weather elements. Although the effect shows up more or less consistently in the long-term averages, it is not reliable enough to depend on every year. Because other sources of large variability are present, the singularity has limited value as a forecasting tool. It serves primarily to focus attention on the potential of the period.

This study was limited to an examination of the January 20–22 singularity in data for the Tennessee area in relation to the regional circulation singularity described by Wahl [1]. How the results fit into the worldwide pattern of January singularities suggested by several recent studies is a tempting question for further speculation. It is interesting to note, for example, that Brier's [6] data on hemispheric fluctuations in the meridional exchange of air at 50° N. latitude, Bowen's [7] rainfall data for a large number of stations in the Northern and Southern Hemispheres, Bigg's [8] high-level cloud data at Australian stations, and Kline and Brier's [9] freezing nuclei counts at Washington, D.C., also were peaked around January 20–24.

REFERENCES

1. E. W. Wahl, "The January Thaw in New England—An Example of a Weather Singularity," *Bulletin of the American Meteorological Society*, vol. 33, No. 9, Nov. 1952, pp. 380–386.
2. Climatological Record Book for Nashville, Tenn., 1931–1950 (unpublished).
3. Unpublished tabulations on file at Weather Bureau Airport Station, Nashville, Tenn., prepared by N. R. Davis.
4. R. D. Fletcher, "The Association of Wind Speed with Height of Upper-Air Constant Pressure Surfaces," *Bulletin of the American Meteorological Society*, vol. 34, No. 4, Apr. 1953, pp. 155–159.
5. U.S. Weather Bureau, Washington, D.C., (a) *Climatological Data, National Summary*, 1950–1958 annual issues; (b) U.S. *Meteorological Yearbook*, issues for 1935–1949; (c) Report of the Chief of the Weather Bureau, 1931–32 to 1933–34.
6. G. W. Brier, "A Note on Singularities," *Bulletin of the American Meteorological Society*, vol. 35, No. 8, Oct. 1954, p. 378.
7. E. G. Bowen, "The Relation Between Rainfall and Meteor Showers," *Journal of Meteorology*, vol. 13, No. 2, Apr. 1956, pp. 142–151.
8. E. K. Bigg, "January Anomalies in Cirriform Cloud Coverage over Australia," *Journal of Meteorology*, vol. 14, No. 6, Dec. 1957, pp. 524–526.
9. D. B. Kline and G. W. Brier, "A Note on Freezing Nuclei Anomalies," *Monthly Weather Review*, vol. 86, No. 9, Sept. 1958, pp. 329–333.

NOTICE

Effective with this issue (January 1959) the 17 climatological charts ordinarily inserted at the end of each issue will be discontinued in the *Monthly Weather Review*. They will continue to be printed (in black and white) in the *Climatological Data, National Summary* which is also issued monthly.

Paid subscribers to the *Review*, who do not already receive the *Climatological Data, National Summary*, will be added to the *CDNS* mailing list for six months or until their present *Review* subscriptions expire, whichever is earlier. Cooperators who need the charts will be placed on the mailing list for the *Climatological Data, National Summary* upon request to Chief, U.S. Weather Bureau, Washington 25, D.C.

U. S. GOVERNMENT PRINTING OFFICE: 1959